

Author Manuscript

1 **Performance of a simple reanalysis proxy for U.S. cloud-to-ground lightning**

2 Michael K. Tippett*

3 *Department of Applied Physics and Applied Mathematics, Columbia University, New York, New*
4 *York*

5 Chiara Lepore
6 *Lamont-Doherty Earth Observatory, Columbia University, Palisades, New York*

7 William J. Koshak
8 *NASA Marshall Space Flight Center, Huntsville, Alabama*

9 Themis Chronis
10 *University of Alabama in Huntsville, Huntsville, Alabama*

11 Brian Vant-Hull
12 *City College of New York, New York City, New York*

13 **This is the author manuscript accepted for publication and has undergone full peer review but**
14 **has not been certified for publication. Copying, distributing, posting, or otherwise making this**
15 **manuscript available online may lead to differences between this version and the Version of Record. Please cite this article**
16 **as doi: [10.1002/joc.6049](https://doi.org/10.1002/joc.6049)**

E-mail: mkt14@columbia.edu

ABSTRACT

16 The product of convective available potential energy (CAPE) and precip-
17 itation rate has previously been used as a proxy for cloud-to-ground (CG)
18 lightning flash counts in climate change applications. Here the ability of this
19 proxy, denoted CP, to represent the climatology and variability of CG light-
20 ning flash counts over the contiguous U.S. (CONUS) during the period 2003–
21 2016 is assessed. CP values computed using the North American Regional
22 Reanalysis are compared with negative and positive polarity CG flash counts
23 from the National Lightning Detection Network. Overall, the proxy performs
24 better on shorter time scales (daily and monthly) than on longer time scales
25 (annual and semi-annual). Proxy performance tends to be worse during the
26 warm season (May–October), when most lightning occurs, and better during
27 the cool season (November–April). The correlation of annually accumulated
28 CONUS CP with CG flash counts is not statistically significant because of
29 poor warm-season performance. Cool season negative CG flash counts are
30 well-correlated with CONUS CP values. Positive CG flash counts ($\sim 7\%$ of
31 all CG flashes) are well correlated with annual values of CONUS CP. The
32 relatively strong relations between CP and CG flash counts in some regions
33 and times of the year at daily resolution provide a benchmark for more com-
34 plex proxies and suggest that proxy-based extended- and long-range predic-
35 tion of lightning activity may be feasible to the extent that precipitation rate
36 and CAPE can be predicted.

37 **1. Introduction**

38 Lightning flash rate is a defining characteristic of thunderstorm evolution. Cloud-to-ground
39 (CG) lightning impacts societies through deaths and injuries, property damage, wildfires, and air
40 quality (Koshak et al. 2015). The importance of CG lightning is a motivation for studying how its
41 characteristics vary under climate change and variability. The relation of lightning with climate,
42 whether in the form of interannual variability or long-term trends, is difficult to infer directly
43 from the observational record because high-quality, spatially complete lightning datasets are often
44 relatively short. Moreover, observational data can at best provide circumstantial information about
45 expected lightning characteristics in climates that differ from the one in which observations are
46 collected, be they future climates or ones in other regions.

47 Lightning activity in general depends on the dynamics and microphysics of convective clouds,
48 and this dependence has been modeled with varying levels of detail and complexity. Lightning
49 occurrence and flash rates can be simulated with considerable fidelity and realism by combining
50 electrification and lightning parameterizations with models of atmospheric dynamics and micro-
51 physics (Mansell et al. 2005; Kuhlman et al. 2006; Fierro et al. 2013). Lightning rates also have
52 been related in a more empirical but effective manner to cloud properties, microphysical param-
53 eters, and updrafts generated by convection permitting models (McCaul et al. 2009; Yair et al.
54 2010; Lynn et al. 2012). Alternatively, lightning flash densities can be diagnosed from the output
55 of convective parameterization schemes in models that do not explicitly resolve clouds (Allen and
56 Pickering 2002; Lopez 2016). Stolz et al. (2017) parameterized storm-scale total lightning density
57 using environmental variables from reanalysis and aerosol data.

58 However, detailed cloud and microphysical properties are not always readily available from
59 reanalysis, seasonal forecasts, or climate change projections, and are themselves uncertain. There-

60 fore, simple proxies for lightning that depend on a few, easily available quantities may provide
61 utility for climate variability and projection applications. Romps et al. (2014) proposed the prod-
62 uct of convective available potential energy (CAPE) and precipitation rate as a proxy for the num-
63 ber of CG lightning flashes. The application of this proxy to climate change projections predicts
64 a 50% increase in United States lightning strokes over the 21st century, which is roughly consis-
65 tent with results for total lightning based on cloud-top height and upward cloud ice flux (Finney
66 et al. 2018). The projected increase in the Romps lightning proxy is driven by robust increases in
67 CAPE, and upward trends in CAPE have been noted in other parts of the world (Murugavel et al.
68 2012). An attractive feature of the Romps proxy is that there is some theoretical understanding of
69 how its constituents are modulated by short-term climate variability (e.g., ENSO; Ropelewski and
70 Halpert 1987; L’Heureux et al. 2015; Allen et al. 2015b) and long-term change (Held and Soden
71 2006; Seeley and Romps 2016). Also, its ingredients are standard outputs of many seasonal and
72 subseasonal dynamical forecasting systems and could be used to make extended-range forecasts
73 of lightning activity (Dowdy 2016; Muñoz et al. 2016). Analogous approaches have been used to
74 relate tornado and hail activity with nearby meteorological quantities at monthly and daily reso-
75 lution (Tippett et al. 2012; Allen et al. 2015a; Tippett et al. 2016; Westermayer et al. 2017). A
76 caveat of empirical proxy-based approaches is that good performance in the current climate does
77 not guarantee good performance in future climates (Stainforth et al. 2007; Camargo et al. 2014).

78 The goal of this work is to assess the extent to which the ingredients of the Romps proxy, pre-
79 cipitation rate and CAPE, capture recent variability in CG flash counts over the contiguous United
80 States (CONUS). Of course, assessing the performance of the proxy in capturing observed CG
81 flash counts is a necessary, but not sufficient requirement for its use in applications such as climate
82 projections and subseasonal to seasonal (S2S) predictions, which is our long-term goal. Import-
83 tantly, good performance with reanalysis in no way guarantees comparable performance in climate

84 projection or S2S forecast applications. On the other hand, poor performance of the proxy in re-
85 analysis would provide useful indications of its limitations. Also, the choice of the Romps proxy
86 is motivated by the availability of CAPE and precipitation rate in forecast and reforecast datasets
87 such as those of the NOAA Climate Forecast System, version 2 (Saha et al. 2014; Lepore et al.
88 2018), the S2S Prediction Project Database (Vitart et al. 2016), and the Subseasonal Experiment
89 (SubX) database (Pegion et al. 2018). However, the CAPE values that are available from forecast
90 models can be sensitive to the choice of parcel and use of the virtual temperature correction.

91 Romps et al. (2014) showed a strong association between daily counts of CONUS CG flashes
92 and the product of CONUS-averages of precipitation rate and CAPE during a single year, 2011.
93 Here we use a longer period (14 years) to see what information is provided by additional years
94 of data regarding seasonal variations in the strength of the association and about the ability of the
95 proxy to capture interannual variability in CG flash counts. Romps et al. (2014) used CAPE cal-
96 culated from radiosonde data and a NOAA River Forecast Centers precipitation product based on
97 rain-gauge and radar data. Here we test the quality of the association between CG flash counts and
98 the CAPE-precipitation product when reanalysis products are used instead of solely observation-
99 based ones. Knowing whether reanalysis products are sufficiently realistic for this application is
100 important because it helps to judge whether such a climate proxy computed from numerical model
101 outputs can be used to forecast or project future CG lightning activity. Furthermore, the use of spa-
102 tially complete reanalysis data allows us to form the product of collocated CAPE and precipitation
103 rate (denoted CP) on a spatially resolved grid and to examine regional features of the association
104 of the CAPE-precipitation product with CG lightning flash counts. A similar study of lightning
105 over Bangladesh, where lightning is an especially dangerous hazard Dewan et al. (2017), found
106 that the CP was more strongly associated with total lightning flash counts during the pre-monsoon
107 season than during the monsoon season (Dewan et al. 2018).

2. Data and methods

a. Data

We use total precipitation rate (mm d^{-1}) and 0-180 hPa most unstable CAPE (J kg^{-1}) data from the North American Regional Reanalysis (NARR; Mesinger and Coauthors 2006). The most unstable parcel is found by dividing the 0-180 hPa layer into six 30-hPa-deep layers and selecting the one with the largest equivalent potential temperature (no virtual temperature correction). NARR data are provided at 3-hourly resolution. The precipitation rate is based on a 3-hour accumulation. CAPE is the instantaneous value at the start of the 3-hour period. The data are averaged from their 32-km native grid spacing to a $1^\circ \times 1^\circ$ latitude-longitude grid. We choose the 1-degree grid spacing to match that of CFSv2 and SubX data because our long-term goal is S2S prediction. NARR precipitation estimates show some advantage over ones from other reanalysis products, especially global reanalysis, likely due to the use of precipitation observations which the NARR assimilates as latent heating profiles (Bukovsky and Karoly 2007; Cui et al. 2017).

Cloud-to-ground (CG) lightning flash counts come from the National Lightning Detection Network (NLDN; Cummins and Murphy 2009) and are summed on the same $1^\circ \times 1^\circ$ grid at daily (UTC) resolution. CG detection efficiency is 90%–95% for CG flashes. Only CONUS land points are used in our analysis, although both NARR and NLDN data extend over ocean and into Mexico and Canada. We use NLDN data covering the period 2003–2016 (5114 days) during which the NLDN network is complete and stable (Koshak et al. 2015). There are 9 days with missing NLDN data: 31/12/03, 08/02/04, 08/02/06, 16/01/07, 06/02/07, 18/12/07, 05/12/08, 17/01/09, 16/01/13, and those days are excluded from calculations. A change in the NLDN Total Lightning Processor (TLP) on 18/09/15 may be responsible for a substantial increase noted in the number of positive CG flashes reported during 2016 (Nag et al. 2016).

131 Negative and positive (≥ 15 kiloampere; kA) polarity CG lightning flash counts are analyzed
132 separately to examine whether the proxy performance differs for positive and negative flash counts.
133 Differing proxy performance might be expected since environment, at least at the mesoscale, can
134 affect storm structure and CG flash polarity (Carey and Buffalo 2007). The total of positive and
135 negative CG flashes were analyzed but give results that are very similar to those for negative CG
136 flash counts. The threshold of 15 kA for positive polarity flashes accounts for the tendency of
137 the NLDN to misclassify cloud pulses as low-amplitude, positive CG strokes (Biagi et al. 2007;
138 Cummins and Murphy 2009). The new NLDN TLP removes the 15 kA peak current limit for
139 positive CG flashes. Therefore, to maintain more consistency, we apply our own 15 kA filter
140 to the positive CG flashes in 2015 and 2016. As a consequence, the numbers of positive CG
141 flashes analyzed here for 2015 and 2016 are less than those in the unfiltered NLDN data sets. The
142 majority (93%) of CONUS CG flashes have negative polarity during the period 2003–2016. The
143 ratio of negative polarity CG flashes to total CG flashes shows substantial spatial variations (Fig.
144 1), with ratios above 95% on the Eastern Seaboard, below 85% in the Upper Midwest, and with
145 the lowest values in very narrow band along the West Coast, consistent with the patterns found
146 in individual years (Koshak et al. 2015). Positive polarity CG flashes have been associated with
147 severe thunderstorms in the Midwest (tornadoes, hail, and damaging wind; e.g., MacGorman and
148 Burgess 1994; Carey and Rutledge 2003). However, other regions with frequent severe weather do
149 not show especially elevated percentages of positive CG flashes. Conversely, the high percentages
150 of positive CG flashes along the West Coast occur where severe weather is infrequent (Zajac and
151 Rutledge 2001; Koshak et al. 2015; Medici et al. 2017).

152 Here we use the product of collocated 3-hourly values of CAPE and precipitation rate as a proxy
153 for the number of CG flashes that occur during those three hours in the corresponding grid cells,
154 and we denote this quantity as CP. Using a proxy based on collocated values allows us to compare

155 it with CG flash counts on a regional as well as CONUS-wide basis. Three-hourly CP values are
156 summed over time to form daily, monthly, seasonal, and annual values; they are summed over
157 space to form regional CONUS values. CP values are scaled to facilitate their comparison with
158 CG flash counts. The scaling factor is computed so that the area-weighted sum of CP values over
159 the period 2003–2016 matches the number of CONUS flashes, depending on polarity. In other
160 words,

$$\text{scaling factor} = \frac{\text{area-weighted sum (CP)}}{\text{sum (CG flashes)}}.$$

161 The scaling factor for negative polarity CG flashes is $64.17 \text{ flashes} / \text{J kg}^{-1} \text{ mm day}^{-1}$ and 4.79
162 $\text{flashes} / \text{J kg}^{-1} \text{ mm day}^{-1}$ for positive polarity CG flashes. On the $1^\circ \times 1^\circ$ grid,

$$\text{CP (scaled to negative CG flash counts)} = 64.17 \times \text{CAPE} \times \text{precipitation} \times \cos \phi,$$

163 and

$$\text{CP (scaled to positive CG flash counts)} = 4.79 \times \text{CAPE} \times \text{precipitation} \times \cos \phi,$$

164 where ϕ is latitude in radians, and $\cos \phi$ accounts for the varying grid cell area. The same scaling
165 factor is used in all months and locations. All comparisons between CP and CG flashes use scaled
166 CP, and we drop the word scaled hereafter.

167 *b. Methods*

168 We assess regional behavior by spatially aggregating CP and CG flashes at the level of NOAA
169 climate regions (Karl and Koss 1984). The states in each region are listed in Supplemental Table
170 S1. The spatial structure of CP and CG flashes are compared using pattern correlations computed
171 for the points east of 105°W with the map mean removed (Wilks 2011). The pattern correla-
172 tions are computed using points east of 105°W to focus on the region where the vast majority of
173 CG flashes are recorded and to avoid giving credit for simply matching the east-west gradient.

174 The temporal association between CP and CG flashes is measured using correlation and mean-
175 squared error (MSE), where the error is the difference of CP and the number of CG flashes. MSE
176 is normalized by the CG flash variance (at the same temporal resolution) to allow comparison
177 of error levels for regions and seasons with disparate levels of CG flash activity. In addition to
178 daily, monthly, and annual aggregation, we also look at totals for six-month warm (May–October)
179 and cool (November–April) seasons, with the cool season consisting of the 13 complete seasons
180 2003/2004–2015/2016 for which data are available. For interannual correlations (14 years), the
181 critical correlation value at the 5% significance level for rejecting the null hypothesis of no corre-
182 lation is about 0.46 for a one-tailed test and 0.53 for a two-tailed test.

183 **3. Results**

184 *a. Regional scaling of CP and CG flashes*

185 Although CP is scaled to match the CONUS total of CG flashes, the ratio of CG flashes to CP
186 shows distinct regional variations (Fig. 2), which presumably reflect the differing frequency of
187 rainfall processes and cloud properties that are not accounted for in CP. Also, the spatial variations
188 in the ratio of CG flashes to CP may indicate a role for additional thermodynamic factors such as
189 wet-bulb temperature (Koshak et al. 2015), mid-level humidity (Westermayer et al. 2017), warm
190 cloud depth (Stolz et al. 2017), or equilibrium level temperature (Bright et al. 2004; Taszarek et al.
191 2017). Deficiencies in reanalysis CAPE might also be a factor (Gensini et al. 2014; King and
192 Kennedy 2019). Values of the ratio of negative CG flashes to CP are slightly above one in the
193 Northeast, where aerosol concentrations are relatively large (van Donkelaar et al. 2015). The ratio
194 of negative flashes to CP is near one east of the Rockies, and substantially greater than one west
195 of 105°W, until along the West Coast where the ratio is much less than one. The picture for pos-

196 itive CG flashes is similar, but without elevated ratio values in the Northeast and with a stronger
197 gradient from values greater than one in the Northern Rockies and Upper Midwest to values less
198 than one in the Southeast. The single scaling factor applied to CP for each polarity matches the
199 behavior in the East because 91.0% of the negative polarity CG flashes and 93.4% of the positive
200 polarity CG flashes occur east of 105°W. Previous studies have noted that ice-based precipita-
201 tion processes are dominant in the arid Southwestern US, and the ratio of convective rainfall to
202 lightning (rainfall yield) is relatively low there (Petersen and Rutledge 1998). Mülmenstädt et al.
203 (2015) found that ice-phase clouds were more frequent in the western half of the CONUS and
204 that liquid-phase clouds were more frequent east of the Rockies. Lower lifted condensation level
205 heights in the East (not shown) are suggestive of lower cloud bases and conditions favoring warm
206 rain processes with greater precipitation efficiency. Fuchs et al. (2015) compared total lightning
207 flash rates in Colorado, Oklahoma, Alabama, and the District of Columbia, and hypothesized that
208 storms with high cloud base heights or shallow warm cloud depths have less warm-phase precipi-
209 tation and more mixed-phase precipitation and lightning. The low ratio of CG flash count to CP in
210 a narrow band along the West Coast may be related to onshore flow of maritime air masses with
211 fewer cloud condensation nuclei or dynamically weaker convection that develops offshore and at
212 coastal boundaries (Zipser 1994; Xu et al. 2012; Holle et al. 2016). Despite some regional scaling
213 deficiencies, CP matches CG flash counts relatively well in the areas where the vast majority of
214 CONUS CG lightning occurs.

215 *b. Daily associations of CONUS totals*

216 We first consider the association of daily CONUS CG flash counts with CAPE alone. The
217 correlation of daily CONUS CG flash counts with CONUS-averaged CAPE from NARR over
218 the period 2003–2016 is larger (values of 0.86 and 0.8, respectively, for counts of negative and

219 positive CG flashes; Fig. 3) than that found by Romps et al. (2014) for CAPE computed from
220 radiosonde data for the single year 2011 ($r = 0.72$). In fact, there is some expectation that reanal-
221 ysis CAPE might be more representative of large-scale features than would be CAPE computed
222 from radiosonde data, since radiosonde data contain small-scale variability that may not be rep-
223 resentative of the large-scale nearby environment. Lepore et al. (2016) found a stronger relation
224 between gauge-measured rainfall extremes and CAPE from reanalysis than with CAPE based on
225 nearby radiosonde measurements. Also, the use of time-averaged reanalysis CAPE and precipi-
226 tation possibly mitigates the difficulty of using observed collocated CAPE and precipitation that
227 is caused by CAPE being released by convection (Romps et al. 2014). On the other hand, daily
228 CONUS-averaged precipitation from NARR shows a slightly weaker relation with CG flash counts
229 (correlation values of 0.36 and 0.43 for negative and positive CG flash counts, respectively; Fig. 3)
230 than the $r = 0.54$ reported by Romps et al. (2014) using a NOAA River Forecast Centers precipita-
231 tion product based on rain-gauge and radar data. Daily CONUS CP has a slightly stronger relation
232 with flash counts (correlation values of 0.89 and 0.87 for negative and positive polarity, respec-
233 tively; Fig. 3) than does CAPE alone. We note that including precipitation rate has the potential
234 to introduce some dependence on aerosols since rain rate increases with aerosol level (Koren et al.
235 2012).

236 *c. Annual cycle and climatology*

237 CONUS CP and CG flash counts have strikingly similar annual cycles, both at daily and monthly
238 resolution, with peak values in summer and much smaller values in the cool season (Fig. 4).
239 The increase in CG occurrence from spring to summer is gradual and followed by a somewhat
240 sharper decay after August (Holle et al. 2016). Annual cycles at daily-resolution are computed by
241 averaging the 14 values (2003–2016) available for each calendar day with February 29 excluded.

242 The daily resolution annual cycle shows that CONUS CP appears to resolve some sub-monthly
243 features that are likely specific to this set of years. The largest discrepancies between the annual
244 cycles of CONUS CP and negative CG flash counts (clearest at monthly resolution) occur in July–
245 August, when CP values are too low, and in September–October when CP values are too high (Fig.
246 4). There is also good agreement between the annual cycles of CONUS CP and positive CG flash
247 counts, with a tendency of CP values to be too low in spring (March–May) and too high in summer
248 and early fall (June–September).

249 The similarity of the annual cycles of CONUS CP and CG flash counts means that some of
250 the variance of CG flash counts at daily resolution explained by CP (Fig. 3) is a consequence of
251 CP accurately capturing the seasonality of CG flash counts. In fact, the annual cycle of CP at
252 daily resolution, a quantity with no year-to-year variation, explains 63% and 52% of the variance
253 of negative and positive daily CONUS CG flash counts, respectively. The annual cycle of CP at
254 daily resolution explains nearly as much variance of daily negative and positive CONUS CG flash
255 counts as do their own annual cycles, which explain 66% and 54%, respectively.

256 CP captures the annual cycle of lightning occurrence at the regional level and monthly resolution
257 to varying degrees (Fig. 5). Because a single (polarity-dependent) factor is used to scale CP,
258 the differing performance of CP in matching the relative magnitude and phasing of the regional
259 seasonal cycles provides another indication of the extent to which CAPE and precipitation alone
260 are adequate to provide a statistical description of CG flash counts. For the most part, both the
261 magnitude of the CG annual cycle and its phasing are well-matched by that of CP in regions east
262 of the Rockies. Because the majority of lightning flashes occur in the eastern half of the country,
263 the scaling factor is disposed to match the magnitude there. In the Upper Midwest, where the
264 ratio of positive to negative CG flashes is relatively large, the CP annual cycle is stronger than
265 that of the negative CG flashes and better matches the annual cycle magnitude of the positive CG

266 flashes. CP overestimates negative CG flashes in the Upper Midwest during July–August and
267 underestimates them in the Plains. The largest differences in annual cycle magnitude are present
268 in the Southwest, Northwest, and West regions, where CP is substantially too low compared to
269 both negative and positive CG flash counts. These annual cycle biases indicate that a lightning
270 proxy potentially could benefit from taking into account physical factors that are different in these
271 regions (e.g., warm cloud depth) and that are not captured by reanalysis precipitation and CAPE.
272 Alternatively, regionally-varying, empirical corrections could be applied to CP as is done to the
273 output of numerical weather and climate prediction models.

274 CP shows the largest phase errors in the Northwest and West. CP in the Northwest peaks in
275 May–June, while CG flash counts peak in June–August and have stronger seasonality (greater
276 peak to trough differences). In the West, CP shows a bimodal structure, with a peak in August and
277 a secondary peak in early spring, while CG flash counts have a unimodal distribution, with a peak
278 in July and stronger seasonality. CP tends to match the annual cycle of positive CG flashes more
279 poorly than it does negative ones, especially in the Southeast, Northeast and Central regions where
280 CP overestimates the peak magnitude.

281 The annual spatial distribution of CP is more similar to that of negative CG flashes than that
282 of positive CG flashes (Fig. 6). The annual spatial distribution of negative CG flashes is nearly
283 indistinguishable from all CG flashes (not shown). Compared to counts of positive CG flashes,
284 corresponding CP values are too low in the middle of the CONUS (Oklahoma, Kansas, and Ne-
285 braska) and too large along the Southeast coast, and over Florida. Centered pattern correlations
286 between the climatological monthly maps of NLDN flash counts and the CP proxy computed for
287 the CONUS region east of 105°W show good agreement for negative polarity flashes throughout
288 the year but are relatively poor for positive CG flashes during June–October (Table 1), which are

289 months when CP values tend to be too high in the Southeast, Northeast, and Central regions and
290 too low in the Plains region (Fig. 5).

291 *d. Seasonality in the strength of daily associations*

292 We compute the correlation between daily CONUS CG flash counts and CP values for each of
293 the twelve calendar months separately to examine how the strength of the association between
294 daily CP values and flash counts varies through the calendar. By removing the mean of each cal-
295 endar month from the daily data, we remove much of the contribution of the annual cycle to the
296 correlation of daily values computed in Section 3b, though some months have considerable clima-
297 tological mean changes within the month (e.g., August). The correlation between daily CONUS
298 CP and CG flash counts by calendar month is very similar for negative, positive, and all polarity
299 flashes (Table 2), and shows a clear seasonality with lower values in summer and fall. The median
300 correlation between daily CONUS CP and all CG flash counts by calendar month is 0.88 during
301 the months of November through May, while it is 0.70 during the months of June through October.

302 The normalized daily MSE shows a consistent picture, with larger relative errors in the months
303 of June through November (Table 2). The daily normalized MSE is relatively low during the
304 months of November through April, with a median of 24% and 36% for negative and positive CG
305 flash counts, respectively. However, during the months of May through October, the median daily
306 normalized MSE is 66% and 65%, respectively, for negative and positive CG flash counts. Nor-
307 malized MSE values greater than one for negative CG flashes in September and October indicate
308 that the errors are greater than would result from replacing the daily CP values with the monthly
309 average over the period. Higher daily errors during the months of peak lightning occurrence might
310 be expected to accumulate and limit the ability of CP to capture year-to-year variations of seasonal
311 and annual totals.

312 *e. Interannual variability*

313 We now examine the ability of CP to match year-to-year variations in monthly, six-month, and
314 annual values of CG flash counts. At annual resolution, there is no substantial correlation of
315 CONUS CP with counts of negative CG flashes ($r = 0.09$; Fig. 7) or with counts of all CG flashes
316 ($r = 0.03$, not shown). To some extent, this lack of association between annual values of CONUS
317 CP and negative CG flashes is unexpected since daily values are well-correlated, both in an overall
318 sense that includes seasonality, and when focusing on individual months. Time averaging often
319 reduces noise and enhances statistical relations, but, in this case, time averaging serves to high-
320 light deficiencies of CP during the warm season. Dewan et al. (2018) also found low correlation
321 of annual numbers of total flashes over Bangladesh with CP, but found a statistically significant
322 relation with CAPE, which is not present here (not shown). The correlation of annual CONUS CP
323 with counts of positive CG flashes is considerably larger ($r = 0.8$; Fig. 7), although that correla-
324 tion drops to 0.52 when the largest annual value (2016) is removed. The large number of positive
325 CG flashes recorded in 2016 could be due to the new flash type classification technique that is
326 based on the examination of multiple waveform parameters, which was employed within the TLP
327 as indicated in Nag et al. (2016).

328 The correlation between warm season (May–October) CONUS CP and CG flashes is roughly the
329 same as for annual values ($r = 0.05$ and $r = 0.76$ for negative and positive polarity, respectively;
330 Fig. 7). Annual counts of CG flashes are dominated by warm season values in the sense that warm
331 season flashes account for 89% of negative CG flashes and 83% of positive CG flashes during
332 the period 2003–2016 (Supplemental Tables S2 and S3) and in the sense that warm season counts
333 of CG flashes are highly correlated with annual values ($r = 0.97$ and $r = 0.99$, for negative and
334 positive flashes, respectively). During the cool season (November–April), CONUS CP shows a

335 fairly good association with negative ($r = 0.74$; Fig. 7), positive ($r = 0.89$; Fig. 7) and all ($r = 0.79$,
336 not shown) CG flash counts. The good association of CONUS CP with the number of CG flashes
337 of both polarities during the cool season is possible because the correlation between the number of
338 negative and positive cool season CONUS CG flashes is 0.69. In contrast, the correlation between
339 the number of negative and positive warm season CONUS CG flashes is -0.32.

340 The correlations of monthly values of CONUS CP with negative CG flashes (first line of Table
341 3) are considerably higher than the annual or warm season correlations, though the correlations for
342 months during the warm season (median correlation 0.47) tend to be lower than for months during
343 the cool season (median correlation 0.87). Correlations of positive CG flash counts with monthly
344 CONUS CP are above 0.85 during six months of the year and fall below 0.5 only in August and
345 October (first line of Table 4), with a tendency toward lower correlations during warm season
346 months (median correlation 0.65) compared to cool season months (median correlation 0.87). The
347 lower correlations during some warm season months is consistent with relatively low correlations
348 and poor normalized MSE at daily resolution during warm season months noted earlier (Table 2).

349 At the regional level, correlations between monthly CP and negative CG flash counts are over-
350 all higher than those at the CONUS level, particularly during warm season months (May through
351 October) when 87% of the regional correlations are greater than CONUS ones (Table 3). Lower
352 correlation with increasing spatial aggregation is consistent with regionally varying magnitude er-
353 rors. Correlations of monthly CP and negative CG flash counts show some indication of relatively
354 lower values in warm season months in the Southeast, Northeast, and South regions, which pro-
355 duce more than 68% of the annual CONUS number of negative CG flashes (Supplemental Table
356 S2). Correlations of monthly CP and positive CG flash counts show some reduced values during
357 warm season months in the South and Southeast regions (Table 4) but are otherwise fairly strong,
358 except in the Central, Upper Midwest, and Plains regions during some cool season months. De-

359 spite clear deficiencies in the South and Southeast regions during the warm season, which likely
360 contribute to poor CONUS performance, the relation between monthly CP and CG flash counts is
361 strong in many regions and during many times of the year, demonstrating the strong potential for
362 CP as an indicator of monthly tendencies in regional CG flash counts.

363 Maps of the correlation between warm and cool season CP and CG flashes show large-scale
364 features that are consistent with the analysis at the NOAA region level, as well as fairly high
365 correlations at the gridpoint level in many areas (Fig. 8). Correlations of warm season CP with
366 negative CG flash counts are mostly positive but very modest in the Southeast, Northeast, and
367 parts of the South, consistent with the regional analysis. Correlations between warm season CP
368 and negative CG flash counts are weakly negative in an area that includes the borders of Colorado,
369 Wyoming, Nebraska, and Kansas where the ratio of intra-cloud lightning to CG flashes is known
370 to be large and which is often associated with inverted or complex charge structures (Carey and
371 Rutledge 1998; Medici et al. 2017). Misclassification of cloud pulses as CG flashes as well as in-
372 correct assignment of first peak polarity have been noted in the Kansas-Nebraska area (Cummins
373 and Murphy 2009). Warm season correlations between CP and negative CG flash counts are also
374 weakly negative in smaller areas along the West Coast, and around Butte, Montana, and Colum-
375 bus, Georgia. Cool season correlations between CP and CG flash counts of both polarities are
376 similar and generally higher than warm season ones across the southeastern half of the CONUS.
377 Correlations between warm season CP and positive CG flashes are overall higher than for negative
378 CG flashes over most of the CONUS, with low correlations mostly limited to Florida and states to
379 its immediate north (Fig. 8). Maps of annual correlations (not shown) are similar to those for the
380 warm season.

381 Warm season normalized MSE exceeds one in many areas for both polarities, indicating errors
382 that are larger than the climatological variance, especially west of 105°W where mean biases are

383 large (Fig. 9). For negative CG flashes, the warm season normalized MSE east of the Rockies is
384 mostly less than one except in areas that include Wisconsin and eastern Minnesota, the Gulf Coast,
385 and eastern North Carolina. On the other hand, the warm season normalized MSE for positive CG
386 flashes is large across the Southeast and Northeast regions, indicating magnitude miscalibration
387 since correlations are good there (Fig. 8). The normalized cool season MSE is lower overall
388 than the warm season MSE for both polarities, except in the Northwest and on the West Coast.
389 Cool season normalized MSE is lower overall for negative CG flashes than for positive ones. Both
390 polarities have large normalized MSE over southern Florida in the cool season. Annual normalized
391 MSE maps (not shown) are similar to warm season ones.

392 4. Summary

393 We have compared the product of collocated CAPE and precipitation (denoted CP) taken from
394 the North American Regional Reanalysis with counts of negative and positive cloud-to-ground
395 (CG) lightning flashes from the National Lightning Detection Network (NLDN) over the con-
396 tiguous U.S. (CONUS). Our analysis includes CONUS-wide and regional characteristics on daily,
397 monthly, and annual resolution for the period 2003–2016. This analysis extends the findings of
398 Romps et al. (2014) who considered one year of CONUS-aggregated daily values from 2011.
399 Overall, the association of CP with lightning flashes on the daily, monthly, and seasonal scale
400 tends to be stronger during the cool season (November–April) than during the warm season (May–
401 October). Interannual correlations between CP and flash counts tend to be stronger for positive
402 CG flashes than for negative ones.

403 Daily values of CONUS CP are highly correlated with both positive and negative CG flash
404 counts, explaining more than 75% of their daily variance (Fig. 3). Some of this association (more
405 than 60% of the variance) is a reflection of the strong seasonal cycles of CONUS CP and CG flash

406 counts and their good phase agreement (Fig. 4). However, daily variations of CONUS CP and CG
407 flash counts with respect to their monthly climatologies are still strongly related, but with stronger
408 associations in the cool season (November–April) than in the warm season (May–October) when
409 most lightning occurs (Table 2). The normalized (relative to climatological variance) daily mean-
410 squared error (MSE) of CONUS values is also larger in the warm season, and this lower accuracy
411 translates into lower interannual correlations (Fig. 7) and higher normalized MSE for monthly
412 totals in the warm season (Table 3), especially for negative polarity flashes, which are the vast
413 majority of CG flashes. The low correlation in summer months might indicate that CP is better
414 related to storm occurrence than to the total number of CG flashes within a storm. This lack of
415 association during the warm season when the majority of lightning occurs results in there being
416 essentially no correlation between the annual values of CP and corresponding numbers of either
417 negative or total CG lightning flashes. There is, however, a good correlation between warm season
418 and annual counts of positive CG flashes with CP (Fig. 7). Cool season CP correlates well with
419 both counts of positive and negative CG flashes.

420 We find that the ratio of CP to CG flash counts varies considerably on a regional basis, with the
421 greatest difference found in the arid Southwest, where the ratio of CG flashes to CP is substantially
422 higher than in between regions east of the Rockies (Fig. 2). The ratio of CG flashes to CP is lowest
423 along the West Coast, where there are fewer cloud condensation nuclei and where maritime air
424 masses can penetrate. At the level of NOAA climate regions, despite some errors in magnitude,
425 CP matches the annual cycle in all regions fairly well except the Northwest and West (Fig. 5).
426 Correlations of annual CP with CG flash counts at the regional level are generally higher for
427 positive than for negative CG flash counts ((Tables 3 and 4). Regional correlations of annual CP
428 and negative CG flash counts are especially low in the South and Northeast, where more than 35%
429 of all negative CONUS CG flashes occur. The relatively weak association between CP and counts

430 of negative CG flashes in these areas during the warm season explains the lack of correlation
431 between annual CONUS CP and negative CG flash counts. In these regions, correlations between
432 cool season CP and CG flash counts are generally stronger than for warm season values. This
433 finding is roughly consistent with those of Dewan et al. (2018) who found higher correlations
434 between CP and total lightning flash count for the pre-monsoon season than for the monsoon
435 season.

436 Maps of the correlation between annual values of CP and CG flash counts show positive values
437 over most of the CONUS, with some spatially limited exceptions (Fig. 8). In general, correlations
438 with CP are stronger for positive CG flash counts and stronger during the cool season for both
439 polarities. Despite the positive correlations at the gridpoint level, interannual variability of CP
440 values are not well-calibrated with CG flash counts. Maps of normalized MSE show relatively
441 low error levels for both polarities during the cool season for most of the CONUS except for large
442 errors on the West Coast, the Northwest, and southern Florida (Fig. 9). Normalized MSE is small
443 during the warm season for positive CG flash counts in a swath that extends from Texas northeast
444 to the Great Lakes.

445 **5. Discussion**

446 The suitability of CP for S2S forecasting applications cannot be concluded from this study.
447 However, assessment with subseasonal reforecast data has been encouraging (Tippett and Koshak
448 2018). In principle, the utility of CP for S2S forecasting is at least limited by its performance with
449 reanalysis data and the extent that its constituents can be forecast. The high correlations between
450 CP and CG flash counts across large portions of the U.S. show that this simple proxy captures
451 considerable variability. Conversely, we have also identified regions and times of the year when
452 CP values are not strongly correlated with CG flash counts, and this weakness suggests the need

453 for improvements in the proxy. The degree to which CP can be predicted in advance is unknown
454 beyond submonthly lead times. There are indications that the CP ingredients, precipitation and
455 CAPE, can be predicted with some skill. U.S. precipitation is already forecast with current forecast
456 systems with some skill at subseasonal (DelSole et al. 2017) and seasonal (Becker et al. 2014)
457 time-scales. However, skill tends to be lowest in the warm season. Seasonal values of CAPE have
458 been demonstrated to be predictable as well (Jung and Kirtman 2016). On the other hand, even
459 in many locations where correlations between CP and CG flash counts are high, the MSE is also
460 relatively high, indicating that the CP proxy is not calibrated to match CG flash counts. In these
461 cases, there is the potential to correct CP values on a regional basis to match CG flash counts.
462 Alternatively, this lack of calibration can also be interpreted as indicating that the proxy can be
463 improved with the addition of other factors that are important for characterizing lightning activity,
464 though perhaps at the risk of losing its attractive simplicity.

465 The 14 years of data used in this study are not adequate to answer fully the question of whether
466 CP is useful proxy for long-term climate applications. Over the period of study, the annual number
467 of CONUS CG flashes varied from a high of 2.7×10^7 flashes in 2004 to a low of 1.8×10^7 flashes
468 in 2012, a range of about 35% of the annual average of 2.3×10^7 flashes. However, this variation
469 in the annual number CONUS CG flashes was not well captured by the CP proxy. This poor
470 performance in describing interannual variability of CONUS CG flash counts does not necessarily
471 mean that this approach is poorly suited to climate change applications but does raise concerns
472 about the applicability of the proxy to climate change applications.

473 *Acknowledgments.* Valuable comments and suggestions from Ken Cummins are gratefully ac-
474 knowledged. M.K.T. and C.L. were partially supported by a Columbia University Research Initia-
475 tives for Science and Engineering (RISE) award; Office of Naval Research awards N00014-12-1-

476 0911 and N00014-16-1-2073; NOAA's Climate Program Office's Modeling, Analysis, Predictions,
477 and Projections program award NA14OAR4310185; and the Willis Research Network.

478 We are also thankful for the support from NASA Program NNH14ZDA001N-INCA (Climate
479 Indicators and Data Products for Future National Climate Assessments; Dr. Jack Kaye and Dr.
480 Lucia Tsaoussi, NASA Headquarters).

481 The authors gratefully acknowledge Vaisala Inc. for providing the NLDN data used in this study.
482 North American Regional Reanalysis data are provided by the NOAA/OAR/ESRL PSD, Boulder,
483 Colorado, USA from their website at <http://www.esrl.noaa.gov/psd> and the Data Support Section
484 of the Computational and Information Systems Laboratory at the National Center for Atmospheric
485 Research (NCAR). NCAR is supported by grants from the National Science Foundation.

486 The authors declare no conflict of interest.

487 **Supporting information**

488 **Table S1.** States in NOAA climate regions.

489 **Table S2.** Percent of negative NLDN CG flashes occurring in each NOAA region and month
490 2003–2016. Values of 0.00 indicate less than 0.01%.

491 **Table S3.** Percent of positive NLDN CG flashes occurring in each NOAA month 20032016.
492 Values of 0.00 indicate less than 0.01.

493 **References**

494 Allen, D. J., and K. E. Pickering, 2002: Evaluation of lightning flash rate parameterizations for use
495 in a global chemical transport model. *J. Geophys. Res.*, **107**, 4711, doi:10.1029/2002JD002066.

496 Allen, J. T., M. K. Tippett, and A. H. Sobel, 2015a: An empirical model relating U.S. monthly hail
497 occurrence to large-scale meteorological environment. *J. Adv. Model. Earth Syst.*, **7**, 226–243,

498 doi:10.1002/2014MS000397.

499 Allen, J. T., M. K. Tippett, and A. H. Sobel, 2015b: Influence of the El Niño/Southern Oscillation
500 on tornado and hail frequency in the United States. *Nat. Geosci.*, **8**, 278–283, doi:10.1038/
501 ngeo2385.

502 Becker, E., H. v. den Dool, and Q. Zhang, 2014: Predictability and forecast skill in NMME. *J.*
503 *Climate*, **27**, 5891–5906, doi:10.1175/JCLI-D-13-00597.1.

504 Biagi, C. J., K. L. Cummins, K. E. Kehoe, and E. P. Krider, 2007: National Lightning Detection
505 Network (NLDN) performance in southern Arizona, Texas, and Oklahoma in 2003–2004. *J.*
506 *Geophys. Res.*, **112**, D05 208, doi:10.1029/2006JD007341.

507 Bright, D. R., M. S. Wandishin, R. E. Jewell, and S. J. Weiss, 2004: A physically based param-
508 eter for lightning prediction and its calibration in ensemble forecasts. *Preprints, 22nd Conf. on*
509 *Severe Local Storms*, Amer. Meteor. Soc.

510 Bukovsky, M. S., and D. J. Karoly, 2007: A brief evaluation of precipitation from the North
511 American Regional Reanalysis. *J. Hydrometeor.*, **8**, 837–846, doi:10.1175/JHM595.1.

512 Camargo, S. J., M. K. Tippett, A. H. Sobel, G. A. Vecchi, and M. Zhao, 2014: Testing the perfor-
513 mance of tropical cyclone genesis indices in future climates using the HIRAM model. *J. Cli-*
514 *mate*, **27**, 9171–9196, doi:10.1175/JCLI-D-13-00505.1.

515 Carey, L. D., and K. M. Buffalo, 2007: Environmental control of cloud-to-ground lightning polar-
516 ity in severe storms. *Monthly Weather Review*, **135** (4), 1327–1353, doi:10.1175/MWR3361.1,
517 URL <https://doi.org/10.1175/MWR3361.1>.

518 Carey, L. D., and S. A. Rutledge, 1998: Electrical and multiparameter radar observations of a
519 severe hailstorm. *J. Geophys. Res.*, **103**, 13 979–14 000, doi:10.1029/97JD02626.

- 520 Carey, L. D., and S. A. Rutledge, 2003: Characteristics of cloud-to-ground lightning in severe and
521 nonsevere storms over the central United States from 1989–1998. *J. Geophys. Res.*, **108**, 4483,
522 doi:10.1029/2002JD002951.
- 523 Cui, W., X. Dong, B. Xi, and A. Kennedy, 2017: Evaluation of reanalyzed precipitation variability
524 and trends using the gridded gauge-based analysis over the CONUS. *J. Hydrometeor.*, **18**, 2227–
525 2248, doi:10.1175/JHM-D-17-0029.1.
- 526 Cummins, K. L., and M. J. Murphy, 2009: An overview of lightning locating systems: History,
527 techniques, and data uses, with an in-depth look at the U.S. NLDN. *IEEE Trans. Electromagn.*
528 *Compat.*, **51**, 499–518, doi:10.1109/TEMC.2009.2023450.
- 529 DelSole, T., L. Trenary, M. K. Tippett, and K. Pegion, 2017: Predictability of week 3-4 average
530 temperature and precipitation over the contiguous United States. *J. Climate*, **30**, 3499–3512,
531 doi:10.1175/JCLI-D-16-0567.1.
- 532 Dewan, A., M. F. Hossain, M. M. Rahman, Y. Yamane, and R. L. Holle, 2017: Recent
533 lightning-related fatalities and injuries in Bangladesh. *Wea. Climate Soc.*, **9**, 575–589, doi:
534 10.1175/WCAS-D-16-0128.1.
- 535 Dewan, A., E. T. Ongee, R. M., M. M. Rahman, and R. Mahmood, 2018: Lightning activity
536 associated with precipitation and CAPE over Bangladesh. *Int. J. Climatol.*, **38**, 1649–1660, doi:
537 10.1002/joc.5286.
- 538 Dowdy, A. J., 2016: Seasonal forecasting of lightning and thunderstorm activity in tropical and
539 temperate regions of the world. *Sci. Rep.*, **6**, 20 874, doi:10.1038/srep20874.
- 540 Fierro, A. O., E. R. Mansell, D. R. MacGorman, and C. L. Ziegler, 2013: The implementation of
541 an explicit charging and discharge lightning scheme within the WRF-ARW model: Benchmark

542 simulations of a continental squall line, a tropical cyclone, and a winter storm. *Mon. Wea. Rev.*,
543 **141**, 2390–2415, doi:10.1175/MWR-D-12-00278.1.

544 Finney, D. L., R. M. Doherty, O. Wild, D. S. Stevenson, I. A. MacKenzie, and A. M. Blyth, 2018:
545 A projected decrease in lightning under climate change. *Nature Climate Change*, **8**, 210–213,
546 doi:10.1038/s41558-018-0072-6.

547 Fuchs, B. R., and Coauthors, 2015: Environmental controls on storm intensity and charge structure
548 in multiple regions of the continental United States. *J. Geophys. Res. Atmos.*, **120**, 6575–6596,
549 doi:10.1002/2015JD023271.

550 Gensini, V. A., T. L. Mote, and H. E. Brooks, 2014: Severe-thunderstorm reanalysis environments
551 and collocated radiosonde observations. *J. Appl. Meteor. Climatol.*, **53**, 742–751, doi:10.1175/
552 JAMC-D-13-0263.1.

553 Held, I. M., and B. J. Soden, 2006: Robust responses of the hydrological cycle to global warming.
554 *J. Climate*, **19**, 5686–5699, doi:10.1175/JCLI3990.1.

555 Holle, R. L., K. L. Cummins, and W. A. Brooks, 2016: Seasonal, monthly, and weekly distri-
556 butions of NLDN and GLD360 cloud-to-ground lightning. *Mon. Wea. Rev.*, **144**, 2855–2870,
557 doi:10.1175/MWR-D-16-0051.1.

558 Jung, E., and B. P. Kirtman, 2016: Can we predict seasonal changes in high impact weather in the
559 United States? *Environ. Res. Lett.*, **11**, 074018, doi:10.1088/1748-9326/11/7/074018.

560 Karl, T. R., and W. J. Koss, 1984: Regional and National Monthly, Seasonal, and Annual Temper-
561 ature Weighted by Area, 1895-1983. Historical climatology series 4-3, National Climatic Data
562 Center, Asheville, NC. 38 pp.

- 563 King, A. T., and A. D. Kennedy, 2019: North American supercell environments in atmospheric
564 reanalyses and RUC-2. *J. Appl. Meteor. Climatol.*, **58**, 71–92, doi:10.1175/JAMC-D-18-0015.1.
- 565 Koren, I., O. Altaratz, L. A. Remer, G. Feingold, J. V. Martins, and R. H. Heiblum, 2012: Aerosol-
566 induced intensification of rain from the tropics to the mid-latitudes. *Nat. Geosci.*, **5**, 118–122,
567 doi:10.1038/ngeo1364.
- 568 Koshak, W. J., K. L. Cummins, D. E. Buechler, B. Vant-Hull, R. J. Blakeslee, E. R. Williams, and
569 H. S. Peterson, 2015: Variability of CONUS lightning in 2003–12 and associated impacts. *J.*
570 *Appl. Meteor. Climatol.*, **54**, 15–41, doi:10.1175/JAMC-D-14-0072.1.
- 571 Kuhlman, K. M., C. L. Ziegler, E. R. Mansell, D. R. MacGorman, and J. M. Straka, 2006: Numer-
572 ically simulated electrification and lightning of the 29 June 2000 STEPS supercell storm. *Mon.*
573 *Wea. Rev.*, **134**, 2734–2757, doi:10.1175/MWR3217.1.
- 574 Lepore, C., M. K. Tippett, and J. T. Allen, 2018: CFSv2 monthly forecasts of tornado and hail
575 activity. *Wea. Forecasting*, **33**, 1283–1297, doi:10.1175/WAF-D-18-0054.1.
- 576 Lepore, C., D. Veneziano, and A. Molini, 2016: Temperature and CAPE dependence of rain-
577 fall extremes in the eastern United States. *Geophys. Res. Lett.*, **42**, 74–83, doi:10.1002/
578 2014GL062247, 2014GL062247.
- 579 L’Heureux, M., M. K. Tippett, and A. G. Barnston, 2015: Characterizing ENSO coupled variabil-
580 ity and its impact on North American seasonal precipitation and temperature. *J. Climate*, **28**,
581 4231–4245, doi:10.1175/JCLI-D-14-00508.1.
- 582 Lopez, P., 2016: A lightning parameterization for the ECMWF Integrated Forecasting System.
583 *Mon. Wea. Rev.*, **144**, 3057–3075, doi:10.1175/MWR-D-16-0026.1.

- 584 Lynn, B. H., Y. Yair, C. Price, G. Kelman, and A. J. Clark, 2012: Predicting cloud-to-ground
585 and intracloud lightning in weather forecast models. *Wea. Forecasting*, **27**, 1470–1488, doi:
586 10.1175/WAF-D-11-00144.1.
- 587 MacGorman, D. R., and D. W. Burgess, 1994: Positive cloud-to-ground lightning in tor-
588 nadic storms and hailstorms. *Mon. Wea. Rev.*, **122**, 1671–1697, doi:10.1175/1520-0493(1994)
589 122<1671:PCTGLI>2.0.CO;2.
- 590 Mansell, E. R., D. R. MacGorman, C. L. Ziegler, and J. M. Straka, 2005: Charge structure and
591 lightning sensitivity in a simulated multicell thunderstorm. *J. Geophys. Res.*, **110**, D12 101,
592 doi:10.1029/2004JD005287.
- 593 McCaul, E. W., S. J. Goodman, K. M. LaCasse, and D. J. Cecil, 2009: Forecasting lightning
594 threat using cloud-resolving model simulations. *Wea. Forecasting*, **24**, 709–729, doi:10.1175/
595 2008WAF2222152.1.
- 596 Medici, G., K. L. Cummins, D. J. Cecil, W. J. Koshak, and S. D. Rudlosky, 2017: The
597 intra-cloud lightning fraction in the contiguous United States. *Mon. Wea. Rev.*, doi:10.1175/
598 MWR-D-16-0426.1.
- 599 Mesinger, F., and Coauthors, 2006: North American Regional Reanalysis. *Bull. Amer. Me-*
600 *teor. Soc.*, **87**, 343–360, doi:10.1175/BAMS-87-3-343.
- 601 Mülmenstädt, J., O. Sourdeval, J. Delanoë, and J. Quaas, 2015: Frequency of occurrence of rain
602 from liquid-, mixed-, and ice-phase clouds derived from A-Train satellite retrievals. *Geophys.*
603 *Res. Lett.*, **42**, 6502–6509, doi:10.1002/2015GL064604.

- 604 Muñoz, Á. G., J. Díaz-Lobato, X. Chourio, and M. J. Stock, 2016: Seasonal prediction of light-
605 ning activity in North Western Venezuela: Large-scale versus local drivers. *Atmos. Res.*, **172–**
606 **173**, 147–162, doi:10.1016/j.atmosres.2015.12.018.
- 607 Murugavel, P., S. D. Pawar, and V. Gopalakrishnan, 2012: Trends of convective available potential
608 energy over the Indian region and its effect on rainfall. *Int. J. Climatol.*, **32**, 1362–1372, doi:
609 10.1002/joc.2359.
- 610 Nag, A., M. J. Murphy, and J. A. Cramer, 2016: Update to the U.S. National Lightning Detection
611 Network. *24th International Lightning Detection Conference & 6th International Lightning Me-*
612 *terology Conference*, San Diego, CA.
- 613 Pegion, K., and Coauthors, 2018: The Subseasonal Experiment (SubX): A multi-model subsea-
614 sonal prediction experiment. *Bull. Amer. Meteor. Soc.*, Submitted.
- 615 Petersen, W. A., and S. A. Rutledge, 1998: On the relationship between cloud-to-ground lightning
616 and convective rainfall. *J. Geophys. Res.*, **103**, 14 025–14 040, doi:10.1029/97JD02064.
- 617 Romps, D. M., J. T. Seeley, D. Vollaro, and J. Molinari, 2014: Projected increase in lightning
618 strikes in the United States due to global warming. *Science*, **346**, 851–854, doi:10.1126/science.
619 1259100.
- 620 Ropelewski, C., and M. Halpert, 1987: Global and regional scale precipitation patterns associated
621 with the El Niño/Southern Oscillation. *Mon. Wea. Rev.*, **115**, 1606–1626.
- 622 Saha, S., and Coauthors, 2014: The NCEP Climate Forecast System Version 2. *J. Climate*, **27**,
623 2185–2208, doi:10.1175/JCLI-D-12-00823.1.

- 624 Seeley, J. T., and D. M. Romps, 2016: Why does tropical convective available potential en-
625 ergy (CAPE) increase with warming? *Geophys. Res. Lett.*, **42**, 10 429–10 437, doi:10.1002/
626 2015GL066199.
- 627 Stainforth, D. A., M. R. Allen, E. R. Tredger, and L. A. Smith, 2007: Confidence, uncertainty and
628 decision-support relevance in climate predictions. *Philos Transact A Math Phys Eng Sci*, **365**,
629 2145–2161, doi:10.1098/rsta.2007.2074.
- 630 Stolz, D. C., S. A. Rutledge, J. R. Pierce, and S. C. van den Heever, 2017: A global lightning
631 parameterization based on statistical relationships among environmental factors, aerosols, and
632 convective clouds in the TRMM climatology. *J. Geophys. Res. Atmos.*, **122**, 7461–7492, doi:
633 10.1002/2016JD026220.
- 634 Taszarek, M., H. E. Brooks, and B. Czernecki, 2017: Sounding-derived parameters associated
635 with convective hazards in europe. *Monthly Weather Review*, **145** (4), 1511–1528, doi:10.1175/
636 MWR-D-16-0384.1, URL <https://doi.org/10.1175/MWR-D-16-0384.1>.
- 637 Tippett, M. K., and W. J. Koshak, 2018: A baseline for the predictability of U.S. cloud-to-ground
638 lightning. *Geophys. Res. Lett.*, **45**, 10,719–10,728, doi:10.1029/2018GL079750.
- 639 Tippett, M. K., C. Lepore, and J. E. Cohen, 2016: More tornadoes in the most extreme U.S.
640 tornado outbreaks. *Science*, **354**, 1419–1423, doi:10.1126/science.aah7393.
- 641 Tippett, M. K., A. H. Sobel, and S. J. Camargo, 2012: Association of U.S. tornado occur-
642 rence with monthly environmental parameters. *Geophys. Res. Lett.*, **39**, L02 801, doi:10.1029/
643 2011GL050368.

- 644 van Donkelaar, A., R. V. Martin, M. Brauer, and B. L. Boys, 2015: Global Annual PM_{2.5} Grids
645 from MODIS, MISR and SeaWiFS Aerosol Optical Depth (AOD), 1998-2012. NASA Socioe-
646 conomic Data and Applications Center (SEDAC), Palisades, NY, doi:10.7927/H4028PFS.
- 647 Vitart, F., and Coauthors, 2016: The subseasonal to seasonal (S2S) prediction project database.
648 *Bull. Amer. Meteor. Soc.*, **98**, 163–173, doi:10.1175/BAMS-D-16-0017.1.
- 649 Westermayer, A. T., P. Groenemeijer, G. Pistotnik, R. Sausen, and E. Faust, 2017: Identification
650 of favorable environments for thunderstorms in reanalysis data. *Meteorol. Z.*, **26**, 59–70, doi:
651 10.1127/metz/2016/0754.
- 652 Wilks, D. S., 2011: *Statistical Methods in the Atmospheric Sciences: An Introduction*. Academic
653 Press.
- 654 Xu, W., R. F. Adler, and N.-Y. Wang, 2012: Improving geostationary satellite rainfall estimates us-
655 ing lightning observations: Underlying lightning–rainfall–cloud relationships. *J. Appl. Meteor.*
656 *Climatol.*, **52**, 213–229, doi:10.1175/JAMC-D-12-040.1.
- 657 Yair, Y., B. Lynn, C. Price, V. Kotroni, K. Lagouvardos, E. Morin, A. Mugnai, and M. d. C.
658 Llasat, 2010: Predicting the potential for lightning activity in Mediterranean storms based on the
659 Weather Research and Forecasting (WRF) model dynamic and microphysical fields. *J. Geophys.*
660 *Res.*, **115**, D04 205, doi:10.1029/2008JD010868.
- 661 Zajac, B. A., and S. A. Rutledge, 2001: Cloud-to-ground lightning activity in the con-
662 tiguous United States from 1995 to 1999. *Mon. Wea. Rev.*, **129**, 999–1019, doi:10.1175/
663 1520-0493(2001)129<0999:CTGLAI>2.0.CO;2.
- 664 Zipser, E. J., 1994: Deep cumulonimbus cloud systems in the Tropics with and without lightning.
665 *Mon. Wea. Rev.*, **122**, 1837–1851, doi:10.1175/1520-0493(1994)122<1837:DCCSIT>2.0.CO;2.

666 **LIST OF TABLES**

667 **Table 1.** Centered pattern correlation between climatological CP and NLDN CG flash
 668 counts east of 105°W. 32

669 **Table 2.** Correlation and normalized MSE of daily CONUS CP and NLDN values
 670 pooled by month. 33

671 **Table 3.** Correlation of monthly averages of negative NLDN flash counts and CP. Low-
 672 skill values (less than 0.5) are indicated in bold. Correlation of annual average
 673 are provided in the final column. 34

674 **Table 4.** Correlation of monthly averages of positive NLDN flash counts and CP. Low-
 675 skill values (less than 0.5) are indicated in bold. Correlation of annual average
 676 are provided in the final column. 35

TABLE 1. Centered pattern correlation between climatological CP and NLDN CG flash counts east of 105°W.

Polarity	J	F	M	A	M	J	J	A	S	O	N	D
Total	0.89	0.90	0.95	0.96	0.94	0.88	0.85	0.86	0.80	0.78	0.91	0.92
Negative	0.88	0.90	0.95	0.96	0.94	0.87	0.84	0.85	0.80	0.78	0.90	0.91
Positive	0.89	0.87	0.92	0.95	0.88	0.68	0.51	0.67	0.69	0.75	0.90	0.91

TABLE 2. Correlation and normalized MSE of daily CONUS CP and NLDN values pooled by month.

Correlation												
Polarity	J	F	M	A	M	J	J	A	S	O	N	D
All	0.87	0.90	0.89	0.90	0.86	0.74	0.69	0.68	0.70	0.71	0.80	0.88
Negative	0.87	0.90	0.89	0.89	0.85	0.73	0.67	0.66	0.69	0.70	0.79	0.87
Positive	0.88	0.90	0.87	0.89	0.86	0.70	0.66	0.68	0.73	0.72	0.83	0.90
Normalized MSE												
Polarity	J	F	M	A	M	J	J	A	S	O	N	D
All	0.24	0.21	0.22	0.21	0.37	0.60	0.62	0.63	1.08	0.99	0.66	0.23
Negative	0.25	0.21	0.23	0.23	0.40	0.61	0.65	0.66	1.11	1.03	0.74	0.29
Positive	0.40	0.39	0.33	0.27	0.29	0.67	0.64	0.64	0.77	0.66	0.32	0.42

677

678

TABLE 3. Correlation of monthly averages of negative NLDN flash counts and CP. Low-skill values (less than 0.5) are indicated in bold. Correlation of annual average are provided in the final column.

Region	J	F	M	A	M	J	J	A	S	O	N	D	Annual
CONUS	0.85	0.90	0.88	0.84	0.51	0.66	0.36	0.34	0.46	0.81	0.84	0.96	-0.09
South	0.74	0.87	0.76	0.76	0.66	0.32	0.41	0.34	0.63	0.65	0.63	0.87	0.02
Southeast	0.90	0.91	0.91	0.82	0.87	0.85	0.76	0.45	0.74	0.88	0.95	0.95	0.67
Northeast	0.67	0.94	0.91	0.88	0.72	0.83	0.65	0.52	0.62	0.75	0.87	0.91	0.16
Central	0.48	0.42	0.91	0.20	0.83	0.85	0.88	0.56	0.76	0.93	0.80	0.38	0.62
Upper Midwest	0.50	0.71	0.95	0.79	0.63	0.77	0.75	0.72	0.65	0.92	0.74	0.61	0.56
Plains	0.11	0.88	0.94	0.91	0.63	0.61	0.43	0.74	0.85	0.59	0.60	0.06	0.11
Southwest	0.65	0.75	0.90	0.90	0.90	0.83	0.60	0.60	0.59	0.93	0.79	0.35	0.74
Northwest	0.40	0.32	0.29	0.61	0.72	0.90	0.70	0.94	0.97	0.43	0.36	0.71	0.60
West	0.84	0.78	0.27	0.61	0.80	0.81	0.75	0.92	0.85	0.86	0.27	0.43	0.64

679

680

TABLE 4. Correlation of monthly averages of positive NLDN flash counts and CP. Low-skill values (less than 0.5) are indicated in bold. Correlation of annual average are provided in the final column.

Region	J	F	M	A	M	J	J	A	S	O	N	D	annual
CONUS	0.86	0.96	0.86	0.85	0.66	0.64	0.72	0.48	0.80	0.41	0.87	0.97	0.80
South	0.59	0.90	0.77	0.75	0.83	0.49	0.41	0.22	0.70	0.41	0.63	0.96	0.43
Southeast	0.93	0.92	0.84	0.82	0.83	0.50	0.56	0.41	0.59	0.56	0.90	0.93	0.67
Northeast	0.80	0.96	0.92	0.96	0.64	0.93	0.80	0.66	0.82	0.71	0.97	0.98	0.87
Central	0.61	0.31	0.88	0.25	0.89	0.92	0.88	0.81	0.98	0.88	0.77	0.40	0.89
Upper Midwest	0.32	0.79	0.82	0.95	0.91	0.92	0.81	0.72	0.90	0.90	0.74	0.49	0.81
Plains	0.25	0.95	0.92	0.96	0.84	0.79	0.88	0.80	0.90	0.40	0.67	0.17	0.80
Southwest	0.76	0.79	0.96	0.92	0.84	0.64	0.50	0.82	0.50	0.91	0.79	0.15	0.59
Northwest	0.88	0.57	0.71	0.60	0.59	0.90	0.83	0.93	0.97	0.73	0.65	0.88	0.67
West	0.86	0.81	0.47	0.62	0.66	0.94	0.88	0.86	0.84	0.89	0.58	0.51	0.64

681 **LIST OF FIGURES**

682 **Fig. 1.** Ratio in percent of the number of negative polarity CG flashes to the total number of CG
683 flashes 2003–2016. 37

684 **Fig. 2.** Ratio of the number of negative polarity (left) and positive polarity (right) NLDN flash
685 counts to CP. 38

686 **Fig. 3.** Scatter plots of daily values of the CONUS-average of CAPE (first column), precipitation
687 rate (second column), and scaled CP (third column) with daily counts of negative (first row)
688 and positive (second row) CG flashes. Correlation values and 95% bootstrap confidence in-
689 tervals (10,000 bootstrap samples) are shown in the legend. Blue dashed lines are regression
690 lines, and red dashed lines in the right two panels are the one-to-one lines. 39

691 **Fig. 4.** Annual cycles of CP and NLDN CG flash counts at daily (top row) and monthly (bottom
692 row) resolution for negative (left column) and positive (right column) polarity. 40

693 **Fig. 5.** Regional climatology for NOAA climate regions. Upper panels are for negative CG flash
694 counts and lower panels are for positive CG flash counts. The correlation is given in paren-
695 theses. 41

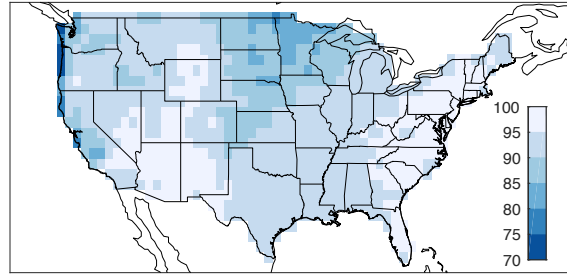
696 **Fig. 6.** Annual averages of negative and positive polarity lightning flashes and the corresponding
697 maps of CP. 42

698 **Fig. 7.** Time series 2003–2016 of annual (first column), warm season (May–October; second col-
699 umn) and cool season (November–April; third column) values of CP and NLDN CG flash
700 counts for negative polarity (first row) and positive polarity (second row). Correlation values
701 and 95% bootstrap confidence intervals (10000 bootstrap samples) are shown in the titles. . . . 43

702 **Fig. 8.** Correlation of CP with negative (top row) and positive (bottom row) CG flashes during
703 the warm (May–October; left column) and cool (November–April; right column) seasons
704 2003–2016. 44

705 **Fig. 9.** Normalized (relative to climatological variance) MSE of the difference of CP with negative
706 (top row) and positive (bottom row) CG flashes during the warm (May–October; top row)
707 and cool (November–April; bottom row) seasons 2003–2016. 45

Ratio (%) of negative CG flashes to total 2003-2016



708 FIG. 1. Ratio in percent of the number of negative polarity CG flashes to the total number of CG flashes
709 2003–2016.

Author Manuscript

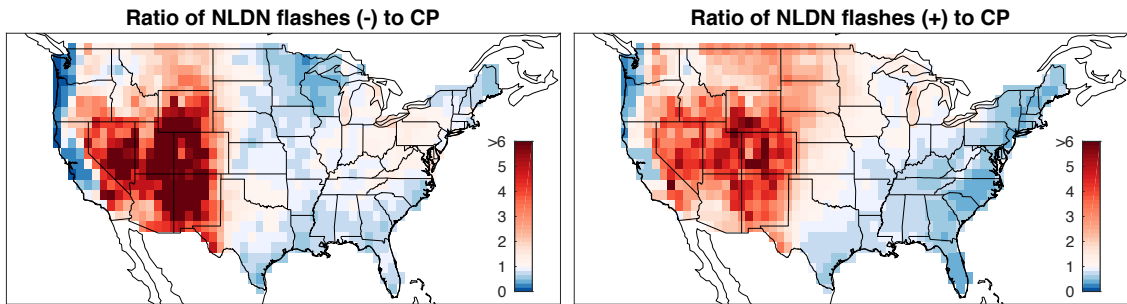
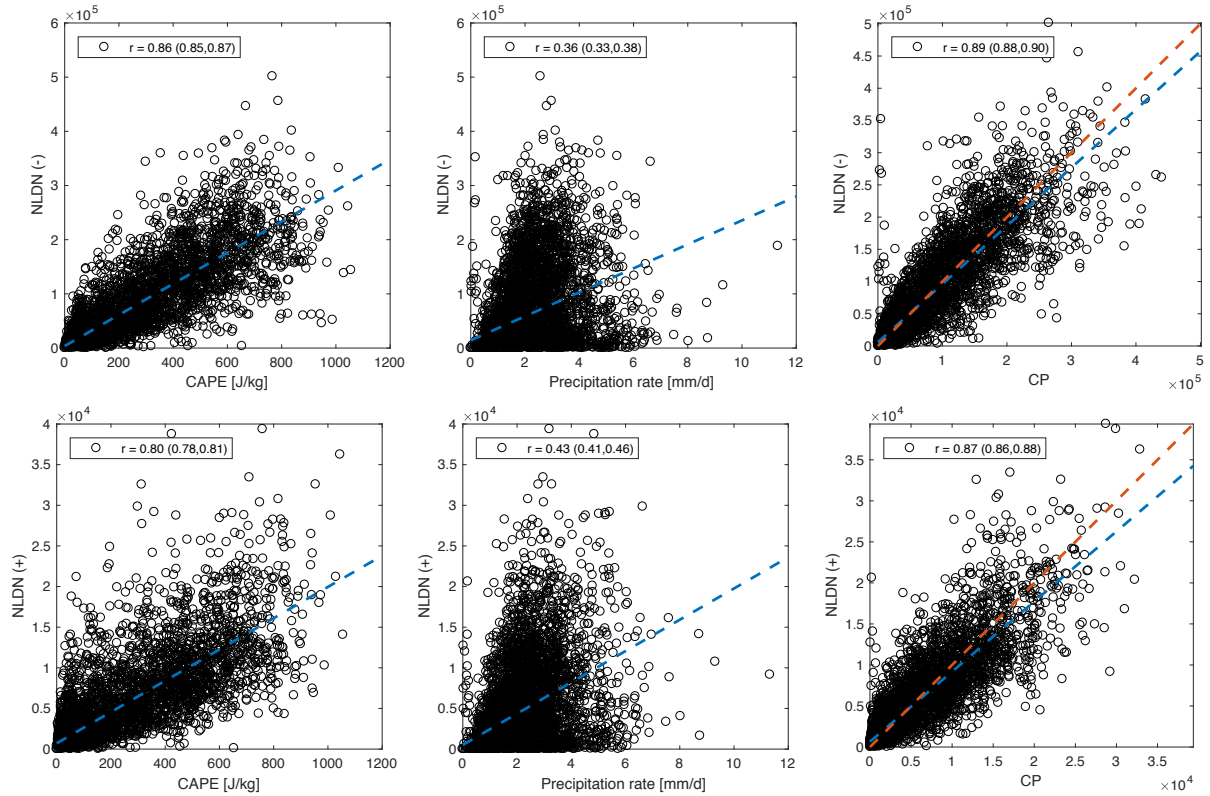
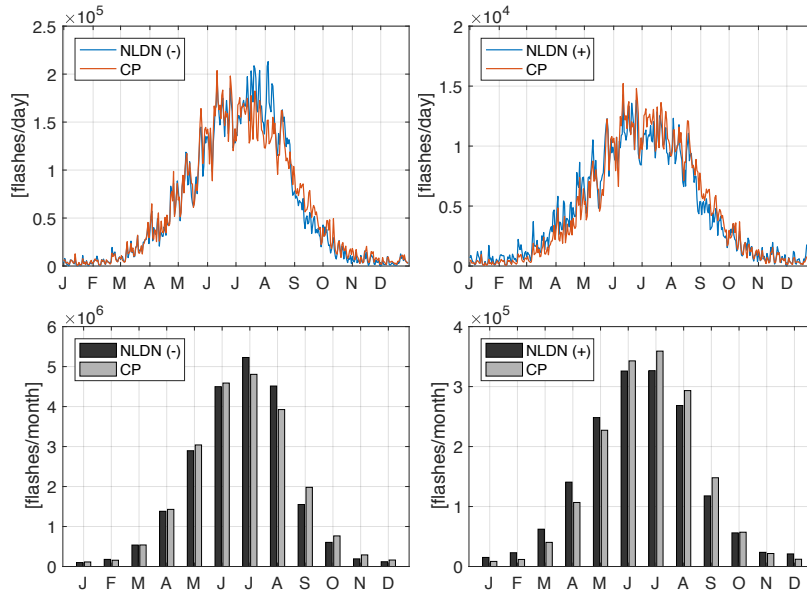


FIG. 2. Ratio of the number of negative polarity (left) and positive polarity (right) NLDN flash counts to CP.

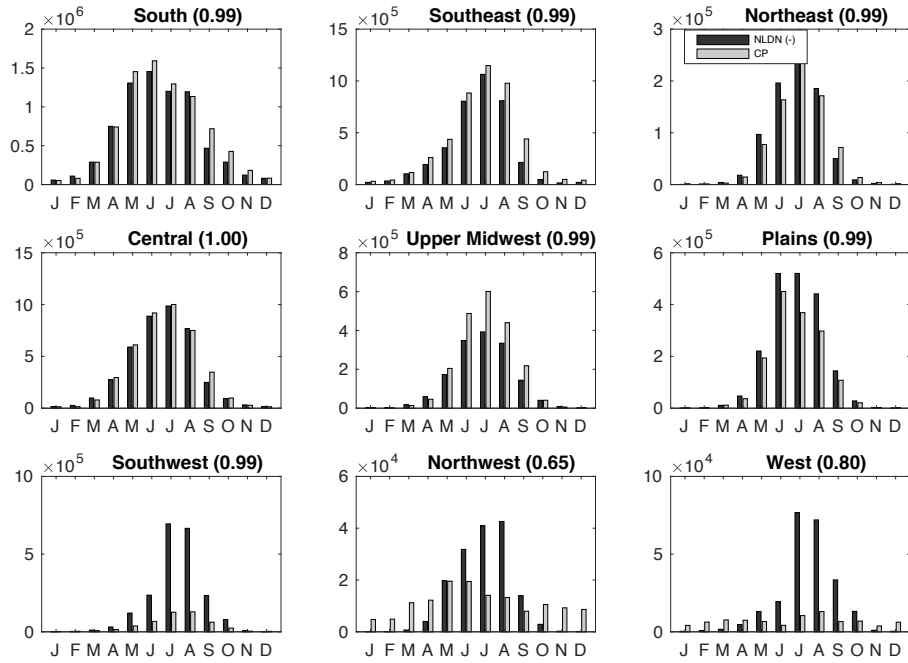


710 FIG. 3. Scatter plots of daily values of the CONUS-average of CAPE (first column), precipitation rate (second
 711 column), and scaled CP (third column) with daily counts of negative (first row) and positive (second row) CG
 712 flashes. Correlation values and 95% bootstrap confidence intervals (10,000 bootstrap samples) are shown in the
 713 legend. Blue dashed lines are regression lines, and red dashed lines in the right two panels are the one-to-one
 714 lines.

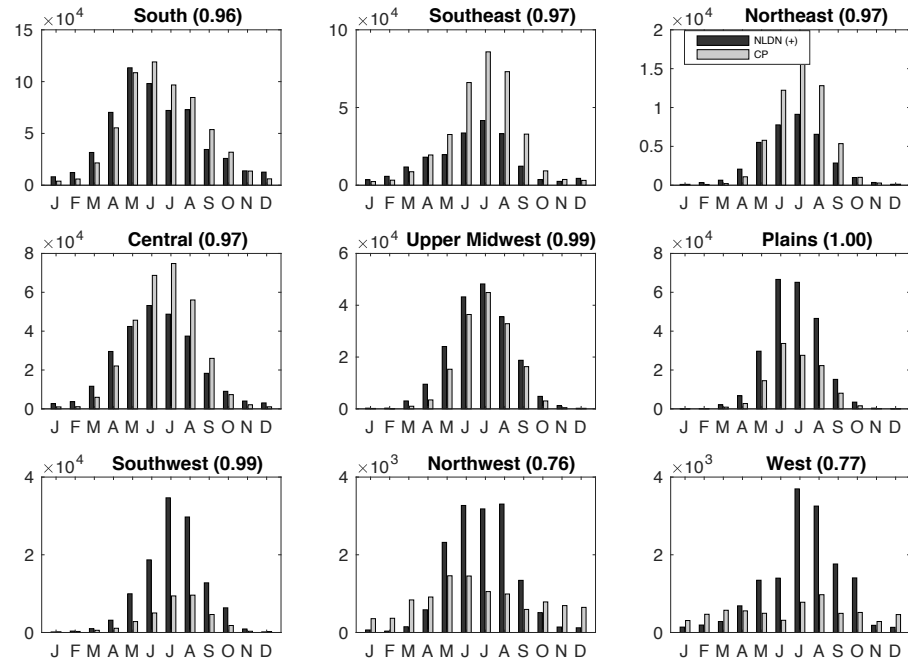


715 FIG. 4. Annual cycles of CP and NLDN CG flash counts at daily (top row) and monthly (bottom row)
 716 resolution for negative (left column) and positive (right column) polarity.

Negative



Positive



717 FIG. 5. Regional climatology for NOAA climate regions. Upper panels are for negative CG flash counts and
 718 lower panels are for positive CG flash counts. The correlation is given in parentheses.

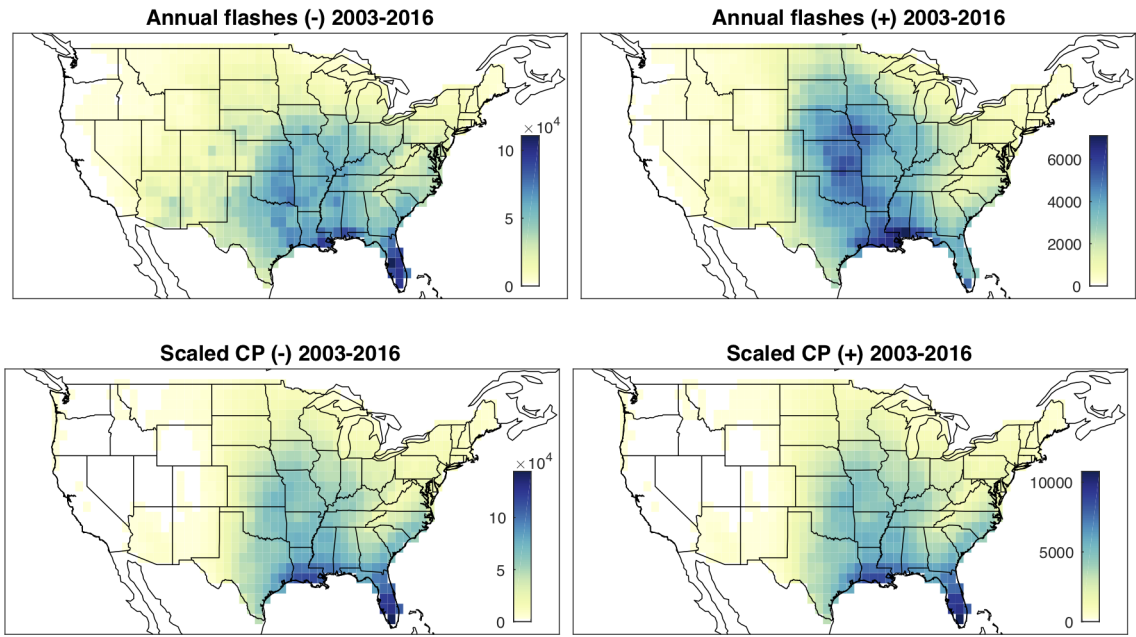
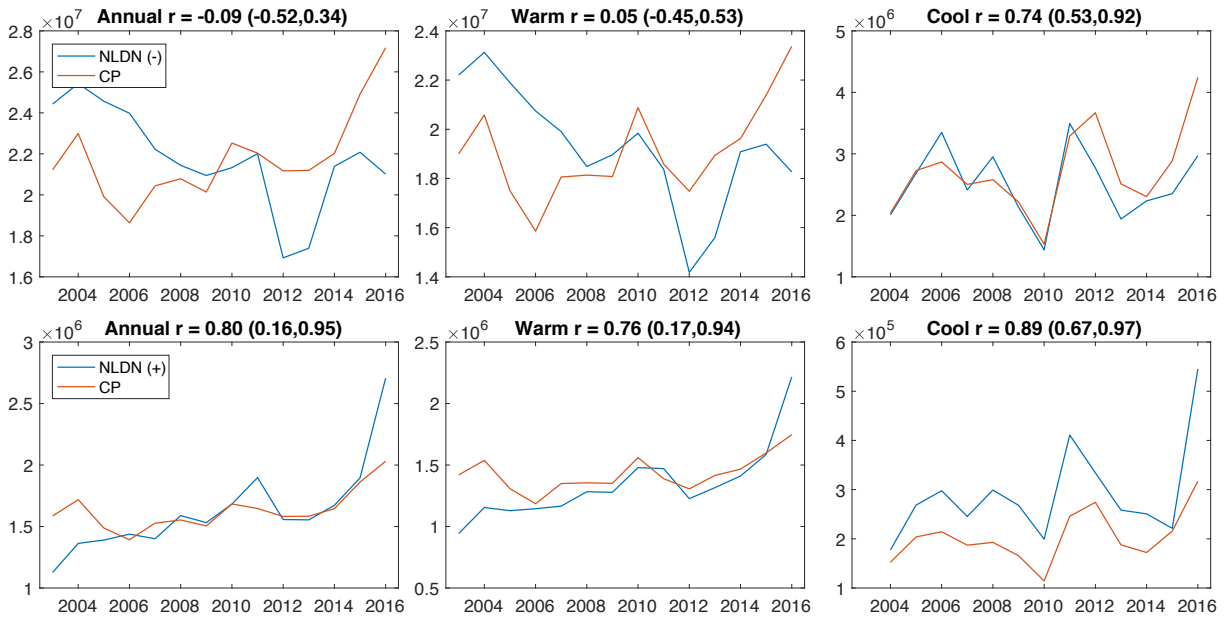
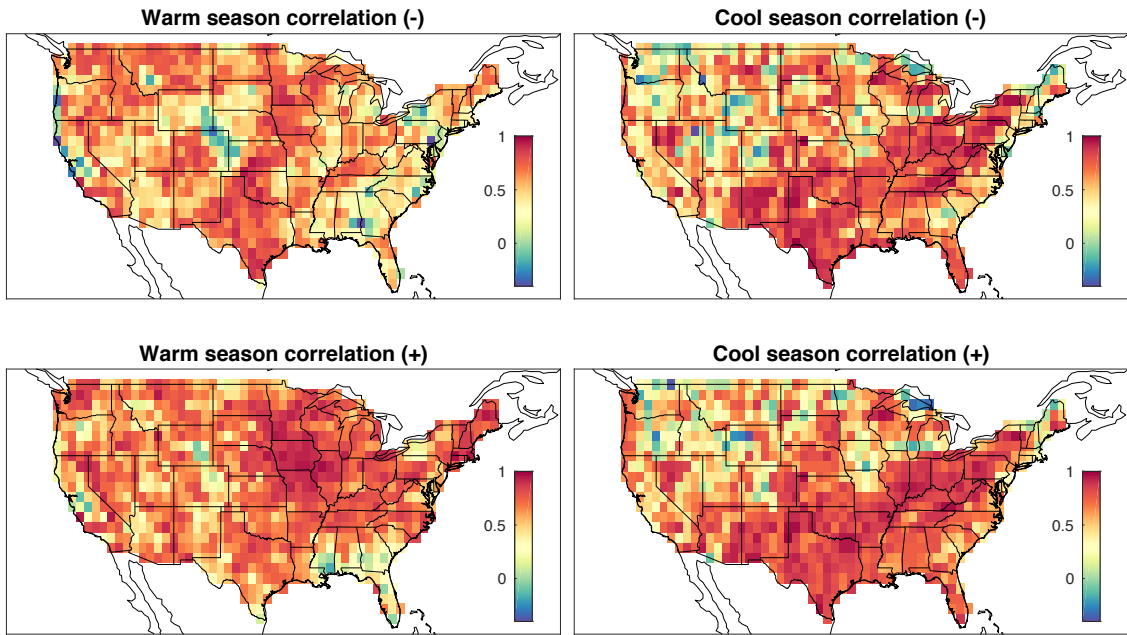


FIG. 6. Annual averages of negative and positive polarity lightning flashes and the corresponding maps of CP.



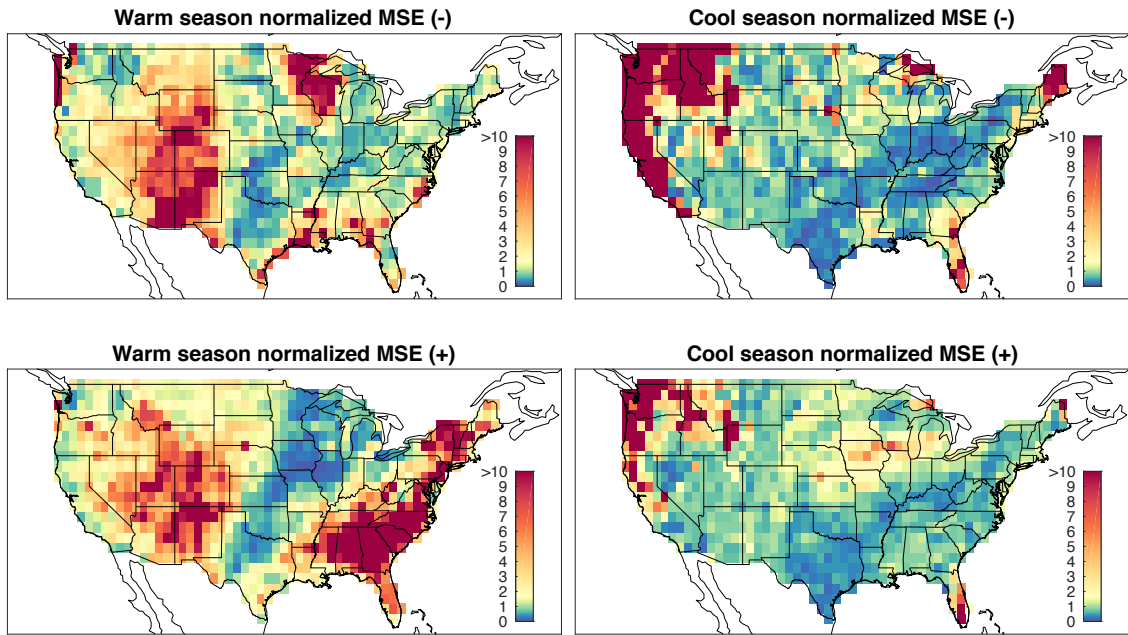
719 FIG. 7. Time series 2003–2016 of annual (first column), warm season (May–October; second column) and
 720 cool season (November–April; third column) values of CP and NLDN CG flash counts for negative polarity
 721 (first row) and positive polarity (second row). Correlation values and 95% bootstrap confidence intervals (10000
 722 bootstrap samples) are shown in the titles.



723

724

FIG. 8. Correlation of CP with negative (top row) and positive (bottom row) CG flashes during the warm (May–October; left column) and cool (November–April; right column) seasons 2003–2016.



725 FIG. 9. Normalized (relative to climatological variance) MSE of the difference of CP with negative (top row)
 726 and positive (bottom row) CG flashes during the warm (May–October; top row) and cool (November–April;
 727 bottom row) seasons 2003–2016.

728 **List of Supporting information tables**

729 **Table S1.** States in NOAA climate regions. 47

730 **Table S2.** Percent of negative NLDN CG flashes occurring in each NOAA region and
731 month 2003–2016. Values of 0.00 indicate less than 0.01%. 48

732 **Table S3.** Percent of positive NLDN CG flashes occurring in each NOAA region and
733 month 2003–2016. Values of 0.00 indicate less than 0.01%. 49

Table S1. States in NOAA climate regions.

South	TX, OK, LA, AR, KS, MS.
Southeast	FL, AL, GA, SC, NC, VA
Northeast	MD, DE, PA, NJ, NY, CT, RI, VT, MA, NH, ME.
Central	TN, MO, IL, IN, OH, KY, WV.
Upper Midwest	IA, MN, WI, MI.
Plains	WY, NE, MT, ND, SD.
Southwest	AZ, NM, UT, CO.
Northwest	OR, ID, WA.
West	CA, NV.

734

Table S2. Percent of negative NLDN CG flashes occurring in each NOAA region and month 2003–2016.

735

Values of 0.00 indicate less than 0.01%.

Region	J	F	M	A	M	J	J	A	S	O	N	D	annual
South	0.10	0.16	0.48	0.89	1.63	3.69	4.88	3.71	0.98	0.22	0.07	0.10	16.92
Southeast	0.26	0.50	1.32	3.44	5.99	6.67	5.50	5.48	2.15	1.33	0.56	0.37	33.58
Northeast	0.08	0.12	0.45	1.26	2.71	4.07	4.53	3.52	1.14	0.42	0.15	0.07	18.52
Central	0.01	0.01	0.08	0.27	0.79	1.60	1.80	1.53	0.66	0.19	0.04	0.00	6.98
Upper Midwest	0.00	0.00	0.05	0.22	1.01	2.39	2.39	2.03	0.66	0.13	0.01	0.00	8.89
Plains	0.00	0.01	0.02	0.08	0.44	0.90	1.16	0.85	0.23	0.04	0.01	0.00	3.75
Southwest	0.00	0.01	0.05	0.14	0.55	1.08	3.19	3.05	1.07	0.36	0.03	0.01	9.56
Northwest	0.00	0.00	0.00	0.02	0.09	0.15	0.19	0.20	0.06	0.01	0.00	0.00	0.72
West	0.00	0.00	0.01	0.02	0.06	0.09	0.35	0.33	0.15	0.06	0.00	0.00	1.09
CONUS	0.45	0.82	2.46	6.34	13.29	20.64	23.98	20.71	7.11	2.77	0.88	0.55	100.00

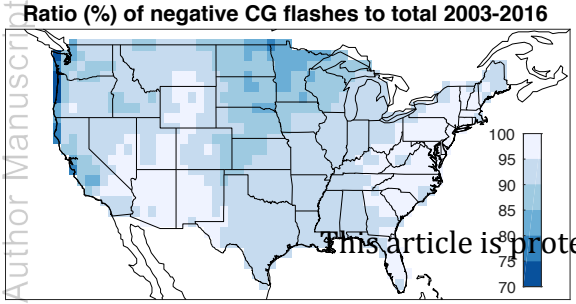
736

Table S3. Percent of positive NLDN CG flashes occurring in each NOAA region and month 2003–2016.

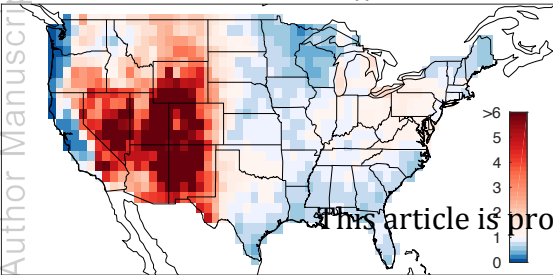
737

Values of 0.00 indicate less than 0.01%.

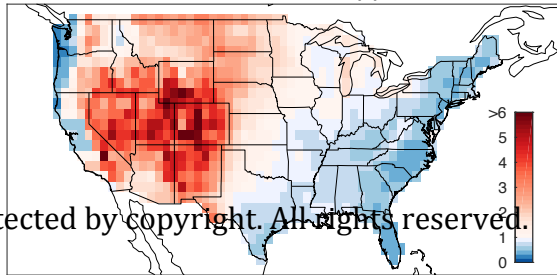
Region	J	F	M	A	M	J	J	A	S	O	N	D	annual
South	0.22	0.35	0.72	1.11	1.21	2.06	2.56	2.04	0.75	0.22	0.15	0.27	11.66
Southeast	0.50	0.75	1.94	4.32	6.96	6.02	4.43	4.47	2.12	1.59	0.85	0.78	34.73
Northeast	0.16	0.23	0.71	1.81	2.60	3.27	2.99	2.30	1.12	0.55	0.25	0.19	16.20
Central	0.02	0.02	0.19	0.58	1.48	2.65	2.96	2.18	1.15	0.30	0.08	0.01	11.62
Upper Midwest	0.00	0.01	0.13	0.41	1.82	4.09	4.00	2.86	0.93	0.21	0.02	0.01	14.50
Plains	0.01	0.02	0.04	0.13	0.34	0.48	0.56	0.40	0.18	0.06	0.02	0.01	2.24
Southwest	0.01	0.02	0.06	0.19	0.61	1.15	2.13	1.83	0.78	0.39	0.06	0.01	7.24
Northwest	0.00	0.00	0.01	0.04	0.14	0.20	0.20	0.20	0.08	0.03	0.01	0.01	0.92
West	0.01	0.01	0.02	0.04	0.08	0.09	0.23	0.20	0.11	0.09	0.01	0.01	0.89
CONUS	0.93	1.41	3.82	8.64	15.25	20.01	20.05	16.48	7.23	3.44	1.45	1.29	100.00



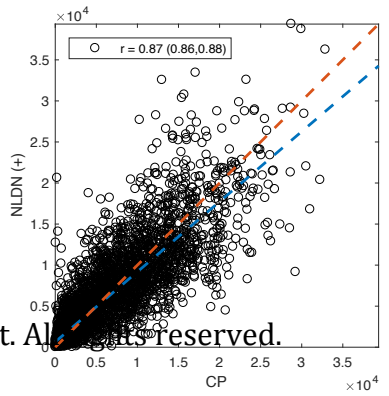
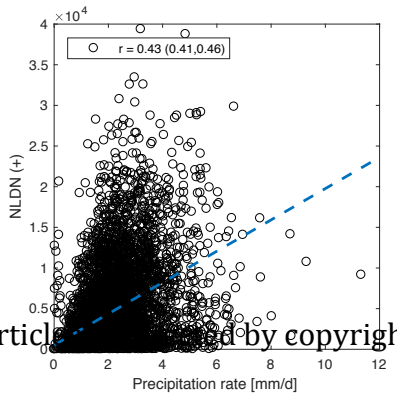
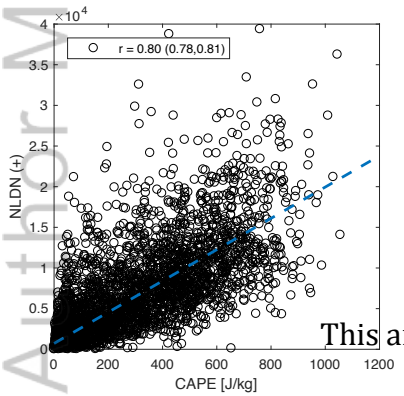
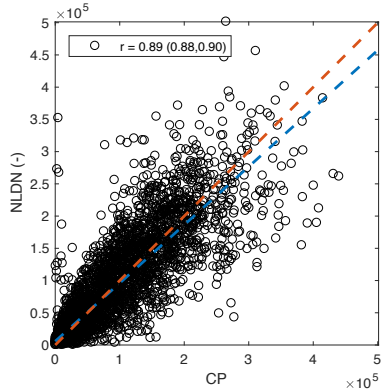
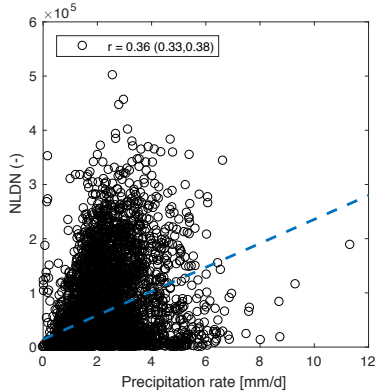
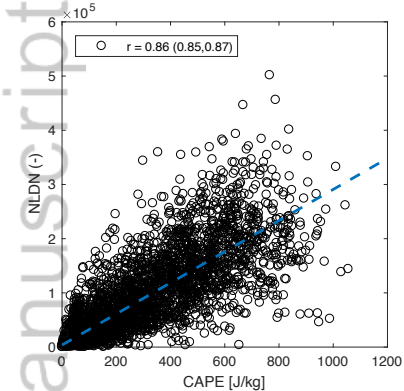
Ratio of NLDN flashes (-) to CP



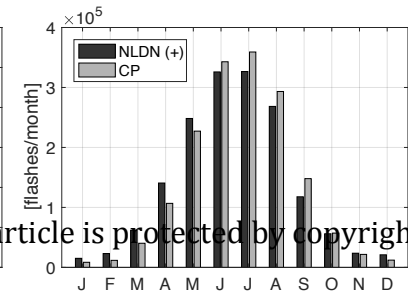
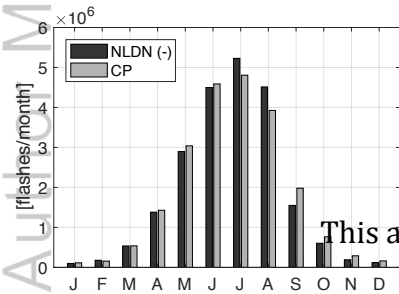
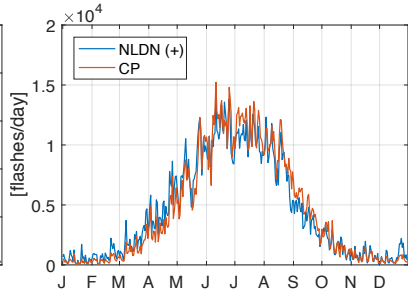
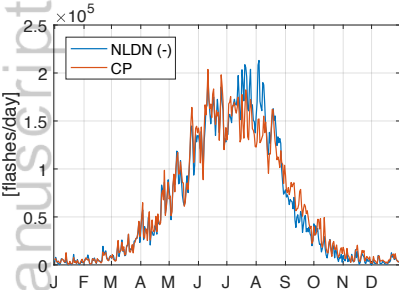
Ratio of NLDN flashes (+) to CP



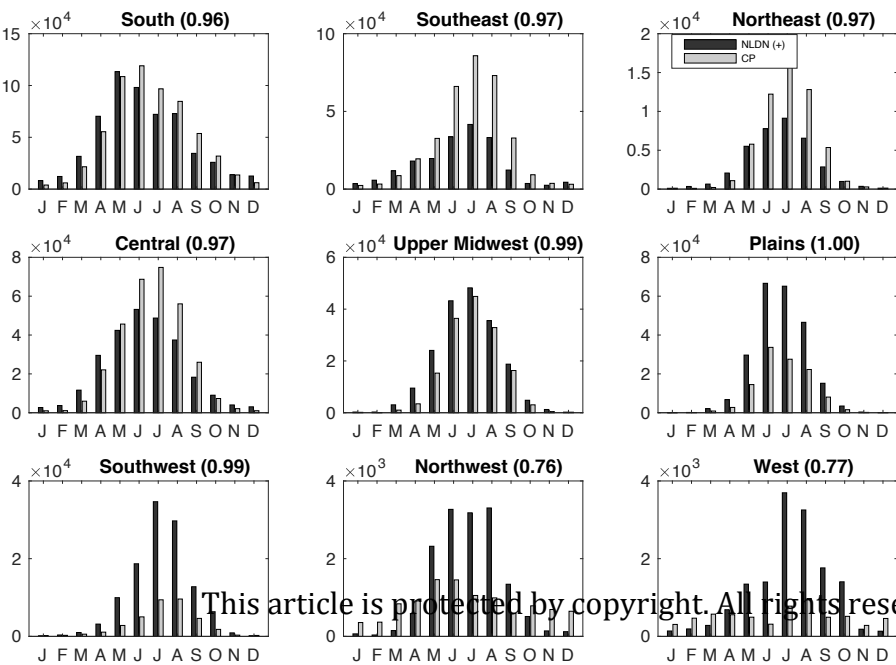
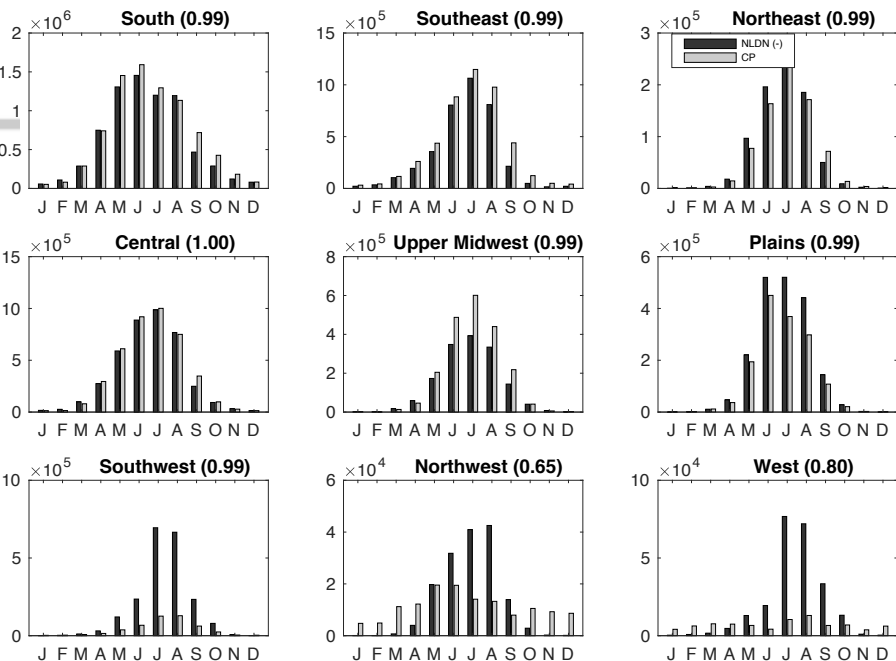
This article is protected by copyright. All rights reserved.



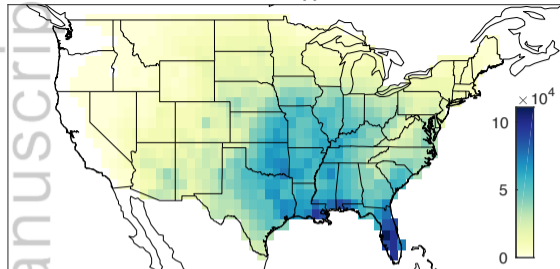
This article is copyrighted by copyright. All rights reserved.



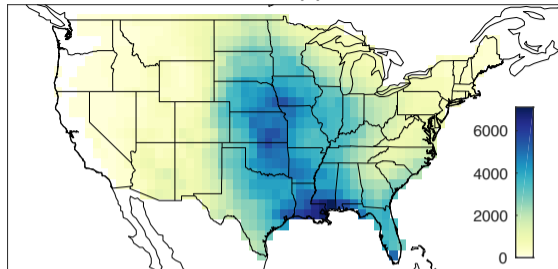
This article is protected by copyright



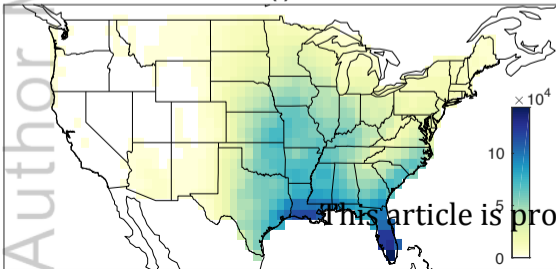
Annual flashes (-) 2003-2016



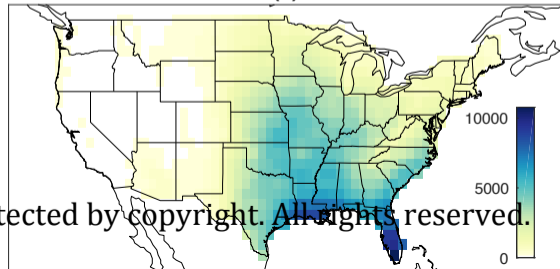
Annual flashes (+) 2003-2016



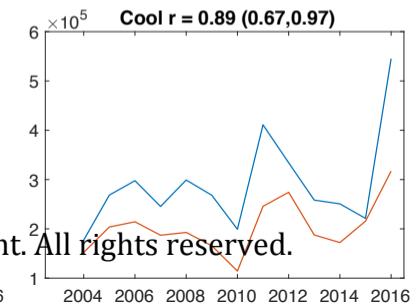
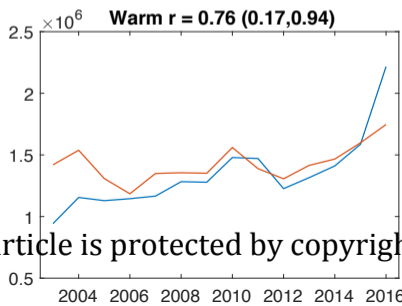
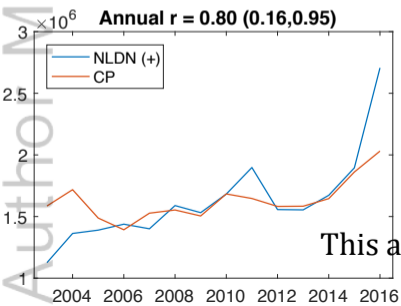
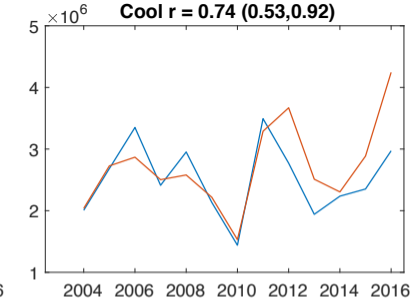
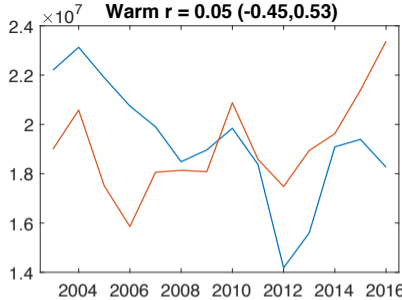
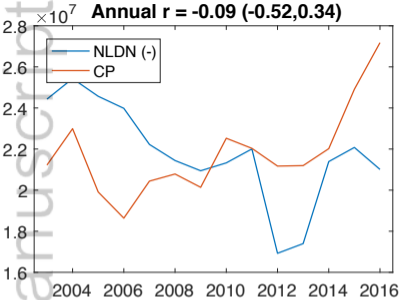
Scaled CP (-) 2003-2016



Scaled CP (+) 2003-2016

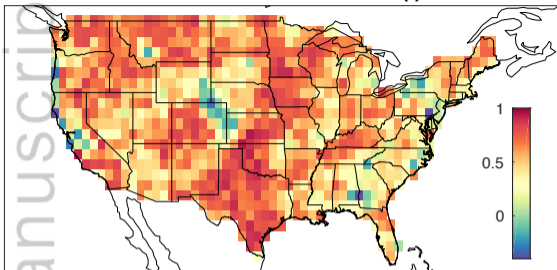


This article is protected by copyright. All rights reserved.

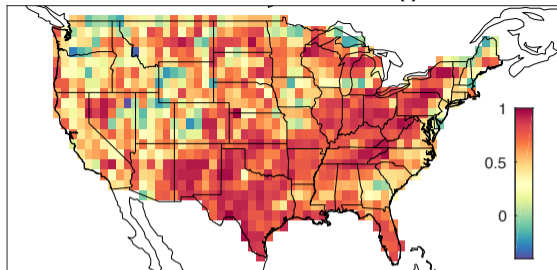


This article is protected by copyright. All rights reserved.

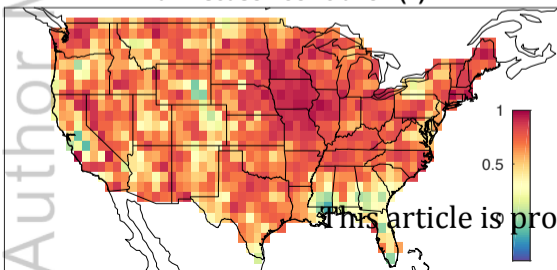
Warm season correlation (-)



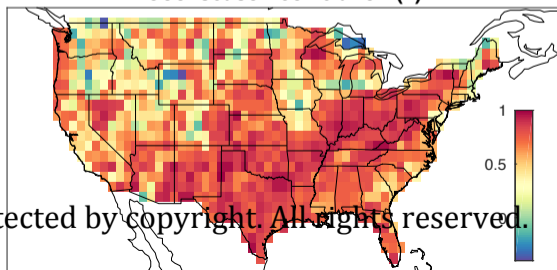
Cool season correlation (-)



Warm season correlation (+)

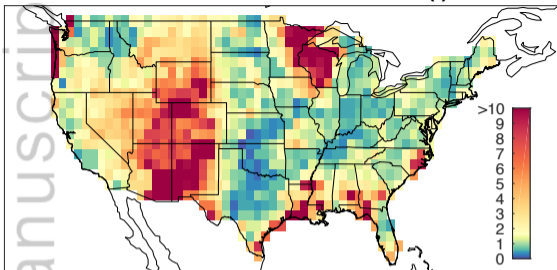


Cool season correlation (+)

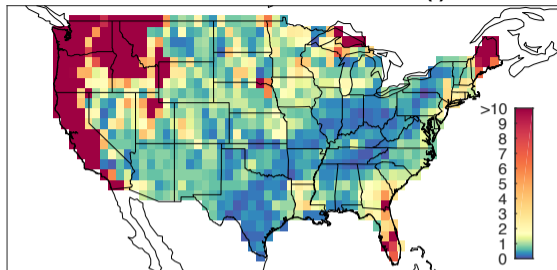


This article is protected by copyright. All rights reserved.

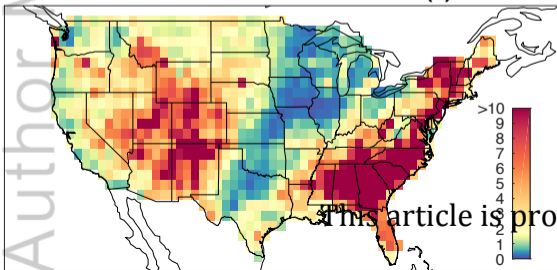
Warm season normalized MSE (-)



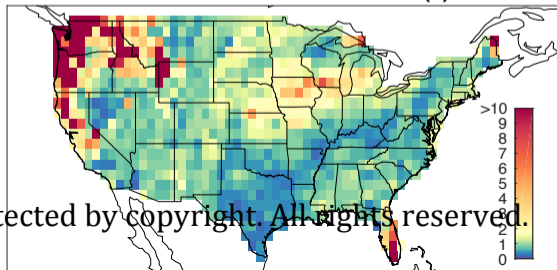
Cool season normalized MSE (-)



Warm season normalized MSE (+)

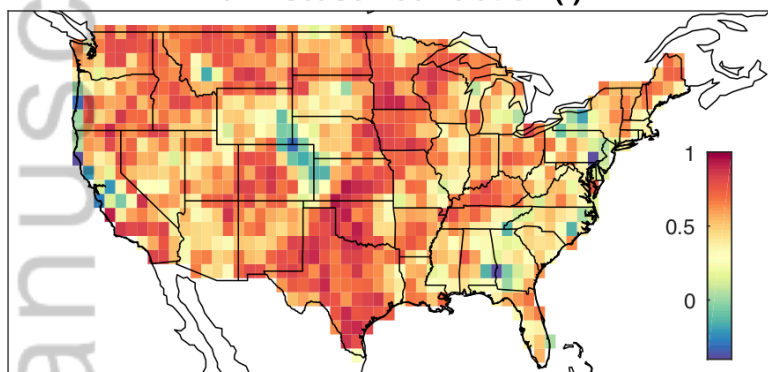


Cool season normalized MSE (+)

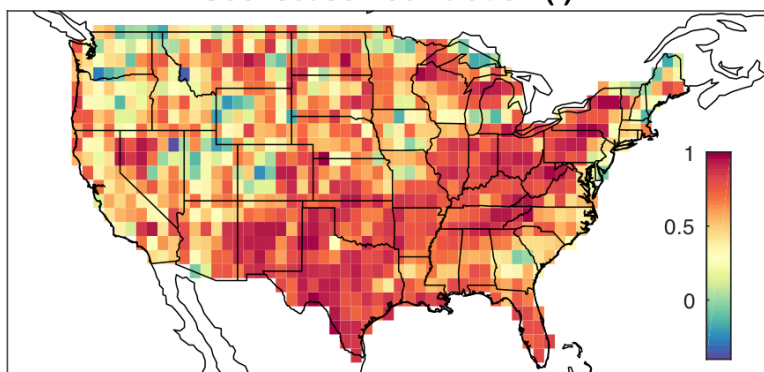


This article is protected by copyright. All rights reserved.

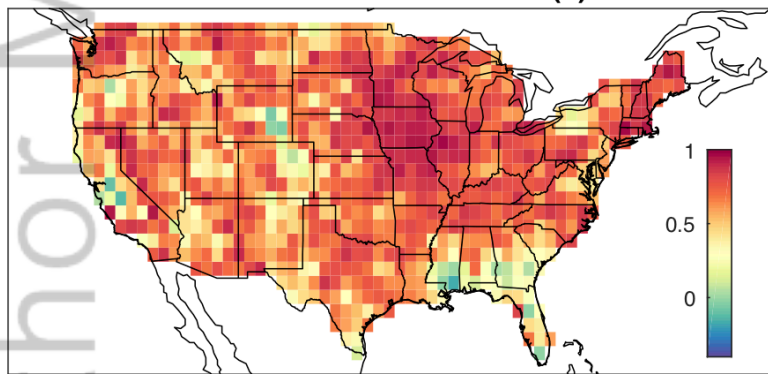
Warm season correlation (-)



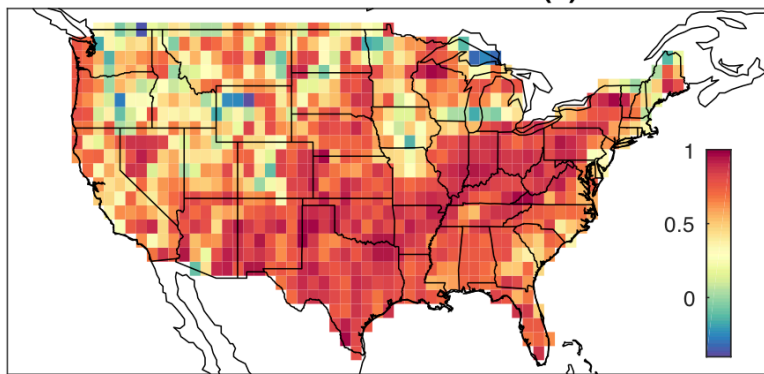
Cool season correlation (-)



Warm season correlation (+)



Cool season correlation (+)



JOC_6049_fig_8.png